

1

Phases and Mesophases

Any process which is not forbidden by a conservation law actually does take place with appreciable probability.

M. Gell-Mann, Il Nuovo Cimento 4, 1956

1.1 Introduction

It takes two antithetic words to indicate *liquid crystals* (LCs) and this gives immediately a hint of the complexity and the fascination of the state of matter that we are about to investigate. Despite this, liquid crystals are not necessarily exotic in their composition or rare in their occurrence, and indeed tens of thousands of liquid-crystalline compounds have been described already.

To start from the very beginning, here we define an equilibrium *phase of matter* as a molecular organization stable within a certain range of thermodynamic variables, e.g. in a certain temperature interval. We are all familiar with the crystalline solid, liquid and gas phases and with their macroscopic properties. For example, we know that crystals have a particular shape that they maintain over time and that they typically have different properties along different directions. Thus, if we measure some optical property of a crystal by sending a beam of light along its different axes we typically find different values. Such a material is accordingly called *anisotropic*. At the other extreme, liquids can flow and take the shape of their container and their physical properties are the same in any direction, thus liquids are *isotropic*. The gaseous state too is isotropic, like a liquid. As we shall see the gas state, except for the density, is indeed very similar to the liquid state, to the point of not being fundamentally distinct from it. On a microscopic level we can imagine an ideal crystal as formed by its constituent particles (molecules or atoms, ions, nanoparticles, ...) with positions regularly arranged on a lattice and, as long as they are non-spherical, with orientations parallel, or however very precisely organized, as shown schematically in Fig. 1.1a. A structure like this is said to possess both *positional* and *orientational order*. In a liquid, molecular positions and orientations are instead disordered overall, as sketched in Fig. 1.1b. We can expect a certain amount of correlations in the positions and orientations of nearby molecules, since each of them will have to adjust to its neighbours to avoid occupying the same space and to optimize attractive interactions. However, this local correlation will rapidly disappear as the separation between molecules increases, so that in

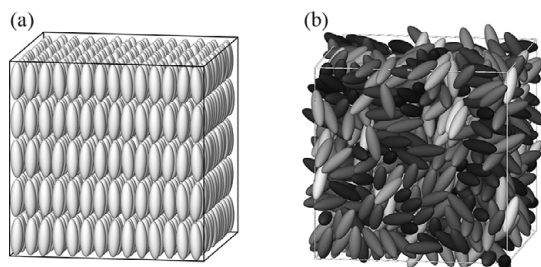
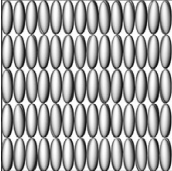
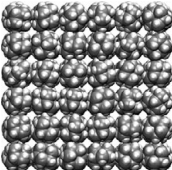
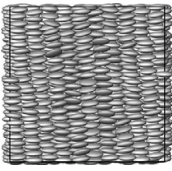
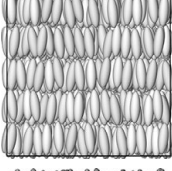
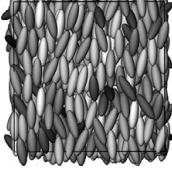
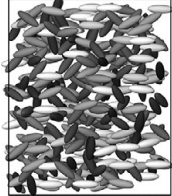
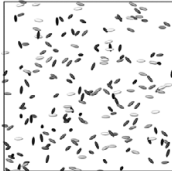


Figure 1.1 (a) A sketch of the molecular organization of a crystal and (b) of an isotropic fluid formed by elongated particles. The grey shade indicates the particles orientation.

an ordinary liquid (or gas) we have no *long range order*. It is apparent that there is a relation between the order at molecular level and the macroscopic properties of a system, and much of this book will be devoted to trying to establish and analyze this connection. It is also worth realizing that there is no rule of nature that forbids the existence of states of matter with long-range order intermediate between that of crystals (three-dimensional positional and orientational) and that of liquids (no positional and no orientational). Since all that is not forbidden can take place in nature or be artificially prepared, we do indeed have a variety of intermediate phases, some examples of which are schematically shown in Table 1.1, with order decreasing from top to bottom. It is reasonable to expect that phases like the *plastic crystal* that have positional, but not orientational, order will be formed by molecules of globular shape that can reorient without disrupting the structure. In practice, tetrahedral (e.g. tetrachloromethane, neopentane), octahedral (e.g. tetramethylbutane), cyclic (cyclobutane), bridged (camphor, adamantane) molecules, etc., give rise to plastic crystals. These rather special crystals have isotropic optical properties and usually they can be easily cut or extruded. Some, e.g. perfluoro cyclohexane, can even flow under their own weight [Kovshev et al., 1977].

When molecules significantly deviate from a globular form, e.g. when they are elongated or discoidal, we have the possibility of phases with orientational order and with a reduced or altogether absent positional order intervening between the crystal and the liquid phases. These intermediate phases or *mesophases* are called *liquid crystals* [de Gennes, 1974; Chandrasekhar, 1992; de Gennes and Prost, 1993; Chaikin and Lubensky, 1995; Collings and Hird, 1997; Khoo, 2007; Blinov, 2011]. Liquid crystals can be obtained from the isotropic liquid by cooling, or from the crystal by heating, and these materials are called *thermotropic*. However, liquid crystal phases can also be formed by mixing a liquid with one or more components formed by anisotropic particles in a suitable concentration range (lyotropics, colloidal suspensions, ...). In the next few sections we shall briefly describe the properties of both families, starting from thermotropics. In these systems the phase transformations can be reversible, with or without hysteresis, and in this case, they are called *enantiotropic* or, as found in a number of materials, the phase transformations take place only in one direction, e.g. upon cooling, and these are called *monotropic*.

Table 1.1. A sketch of the molecular organization of various phases of matter displaying a combination of positional and orientational order

	Phase	Positional order	Orientalional order
	Crystal	Yes, 3D	Yes
	Plastic crystal	Yes, 3D	No
	Columnar LC	Yes, 2D	Yes
	Smectic LC	Yes, 1D	Yes
	Nematic LC	No	Yes
	Liquid	No	No
	Gas	No	No

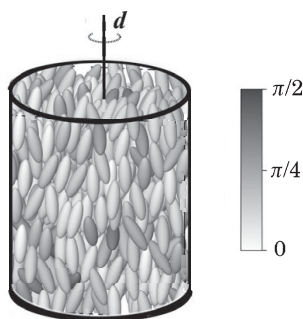


Figure 1.2 Microscopic representation of a nematic monodomain. The molecules tend to be aligned parallel to a common director \mathbf{d} , here along the vertical direction. Their orientation with respect to the director is indicated by the grey level, from white when parallel, to black when perpendicular.

1.2 Nematics

The characteristic property of the molecular organization of nematic liquid crystals is that their molecules tend, on average, to be parallel to one another and to a preferred direction \mathbf{d} , called the *director*. The director at a certain position in space \mathbf{r} can have a different orientation from that at another position \mathbf{r}' , but a nematic can be easily aligned by relatively weak external fields of various kinds: magnetic fields of the order of a few tenths of Tesla, electric fields of the order of Volts per micron [de Gennes and Prost, 1993] or even by surfaces, at least for sufficiently thin layers [Jérôme, 1991], yielding a monodomain sample with a uniform director \mathbf{d} . The resulting aligned nematic, schematically shown in Fig. 1.2, has normally *uniaxial* symmetry around the director, in the sense that its physical properties do not change if we rotate of an arbitrary angle around this direction and here, unless explicitly stated, we shall always assume this to be the case. The properties of nematics are also invariant when we turn a sample upside down, so that \mathbf{d} and $-\mathbf{d}$ are equivalent and, if we consider \mathbf{d} as a unit vector, only its direction will be important. The symmetry of a monodomain nematic can thus be taken to be equivalent to that of a cylinder or, using group theory terminology (see, e.g., [Lax, 1974]), $D_{\infty h}$. This is consistent with molecules forming mesophases (*mesogens*) being apolar or, as is normally the case, being distributed with the same probability along $\pm\mathbf{d}$. The formal description of orientational order will be discussed in detail in Chapter 3, but the tendency of molecules yielding nematics (*nematogens*) to be parallel to \mathbf{d} can be quantified as a first approximation by a simple *order parameter* S first introduced by Tsvetkov [1939]. Consider each mesogen to be a uniaxial object whose orientation is given by a unit vector \mathbf{u}

$$S \equiv \langle P_2 \rangle = \frac{3}{2} \langle (\mathbf{u} \cdot \mathbf{d})^2 \rangle - \frac{1}{2}, \quad (1.1)$$

where $\mathbf{u} \cdot \mathbf{d} \equiv \cos \beta$, with β the angle between the molecular axis and the director, $P_2(\cos \beta)$ is the second Legendre polynomial [Abramowitz and Stegun, 1965] and the angular brackets indicate an average over all the molecules in the system. It is easy to see that $\langle P_2 \rangle$ is a scalar

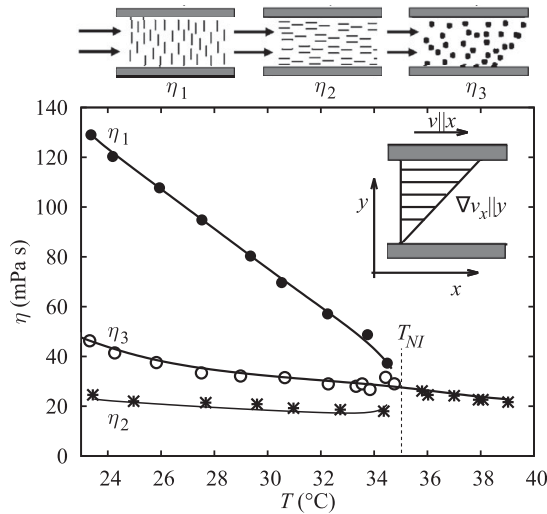


Figure 1.3 The temperature dependence of the Miesowicz shear viscosities η_1, η_2, η_3 for 5CB [Chmielewski, 1986]. In the inset we show a sketch illustrating the definition of these three viscosities [Orr and Pethrick, 2011] for the nematic flowing in a channel with a certain velocity v along x ($v||x$), and a flow velocity gradient across the channel ($\nabla v_x||y$). Each viscosity is measured aligning the director with an external magnetic field H oriented in different directions: $H||d||y$ for η_1 , $H||d||x$ for η_2 and $H||d||z$ for η_3 .

and that it has the properties that we would intuitively expect an order parameter to possess. For a system of molecules perfectly aligned with respect to d , that we take to define our Z laboratory axis, $\beta = 0$ or $\beta = \pi$ for every molecule and $\langle P_2 \rangle = 1$. At the other extreme, for a completely disordered system, such as an ordinary isotropic fluid, we have

$$\langle \cos^2 \beta \rangle = \langle u_Z^2 \rangle = \langle u_X^2 \rangle = \langle u_Y^2 \rangle = \frac{1}{3}, \tag{1.2}$$

since in an isotropic system there will be no preference for any of the three axes and also $u_Z^2 + u_X^2 + u_Y^2 = 1$. Therefore, for a disordered system we have $\langle P_2 \rangle = 0$.

Nematics have long-range orientational order but not long-range positional order and their molecules can move and reorient quite easily, like in a liquid. Indeed the viscosities and the densities of materials in their nematic or isotropic liquid phases are quite similar, typically differing less than 5% on both sides of the transition [Ibrahim and Haase, 1976; Dunmur et al., 2001; Würflinger and Sandmann, 2001]. The orientational order gives, however, different optical, dielectric, diamagnetic and rheological properties in different directions with respect to the director, i.e. a nematic liquid crystal is *anisotropic*. The viscosity itself is different for different relative orientations of the flow velocity v , of the director and of the flow velocity gradient [Miesowicz, 1946], as sketched in Fig. 1.3, where we also plot the three Miesowicz viscosities (η_1, η_2, η_3) for 4-*n*-pentyl-4'-cyano-biphenyl (5CB), showing that the lowest one corresponds to flow along the director (η_2) [Chmielewski, 1986; Orr and Pethrick, 2011].

1.2.1 Optical Properties

Even though the molecules of a nematic tend to arrange parallel to each other, defining a local preferred direction, the director will not point in any specific direction on a macroscopic scale in the absence of a field, for example when we obtain a nematic by cooling from the liquid or melting from the crystal. Rather, its direction will vary continuously so as to maintain on the one hand local uniaxial and on the other macroscopic isotropic symmetry. We can think of the molecules as being aligned within local domains, but with the domains being themselves randomly oriented one with respect to the other. This inhomogeneity gives rise to the scattering of visible light by an unoriented nematic (see Fig. 1.4) and to its characteristic turbid, milky appearance, which disappears at the nematic-isotropic transition, for this reason also called the *clearing* point. In turn, the strong scattering of visible light indicates that local domains leading to birefringence inhomogeneities have dimensions ξ of the order of the wavelength of visible light, i.e. a few hundred nanometres, corresponding to a number of spontaneously correlated molecules of the order of 10^8 . The strong correlation between individual molecules indicated by this huge size is at the origin of the aforementioned easy alignment of nematics under an external field. Indeed a uniform alignment can be obtained by magnetic fields of the order of 0.1 T or, e.g., by electric fields of the order of 1 V/ μm . The free energy contribution corresponding to application of an electric field \mathbf{E} is (see, e.g., [Khoo, 2007])

$$\mathcal{G}_E = -\frac{1}{2} \Delta\epsilon (\mathbf{d} \cdot \mathbf{E})^2. \quad (1.3)$$

The alignment will thus tend to be in the direction of the applied electric field, \mathbf{E} , or perpendicular to it, if the *dielectric susceptibility* anisotropy of the material, $\Delta\epsilon = \epsilon_{\parallel} - \epsilon_{\perp}$,

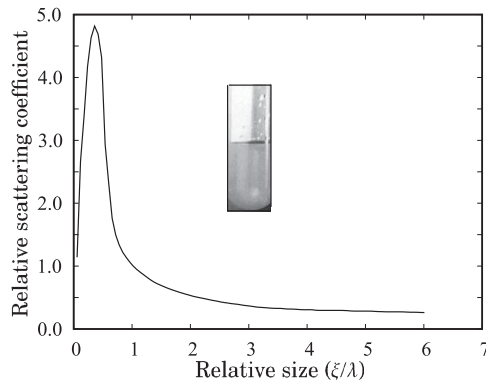


Figure 1.4 Relative scattering coefficient as a function of the ratio between size of the inhomogeneous domains, ξ , and incoming light wavelength λ [Tilley, 2000]. The milky appearance of nematics (inset) indicates that ξ is of the order of a few hundred nanometres, the visible light wavelength.

is positive or negative, respectively. A good alignment will be achieved if this free energy overcomes the thermal disordering energy. In the same way for an applied magnetic field \mathbf{H}

$$\mathcal{G}_B = -\frac{1}{2}\Delta\chi(\mathbf{d}\cdot\mathbf{H})^2, \quad (1.4)$$

where $\Delta\chi$ is the *diamagnetic susceptibility* anisotropy $\Delta\chi = \chi_{\parallel} - \chi_{\perp}$.

An aligned nematic has the optical properties of a uniaxial crystal, like calcite or quartz, with the director representing the optical axis, and shows *birefringence* [Jenkins and White, 2001]. A beam of light, propagating through the sample at an angle with respect to the optical axis, is split in two beams with parallel and perpendicular polarization, corresponding to the refractive indices parallel and perpendicular to the director, n_{\parallel} , n_{\perp} . Thus, in a liquid crystal the refractive index, \mathbf{n} , is a tensor (see Appendix B). In a laboratory fixed system with the z -axis parallel to \mathbf{d} , the 3×3 matrix representing the refractive index tensor will be diagonal, with components $(n_{\perp}, n_{\perp}, n_{\parallel})$. A simple experimental setup for measuring the birefringence, $\Delta n = n_{\parallel} - n_{\perp}$, i.e. the difference between the parallel (or *extraordinary*) and perpendicular (or *ordinary*) components of the refractive index tensor, is shown in Fig. 1.5a. The intensity of a beam of light with wavelength λ emerging through

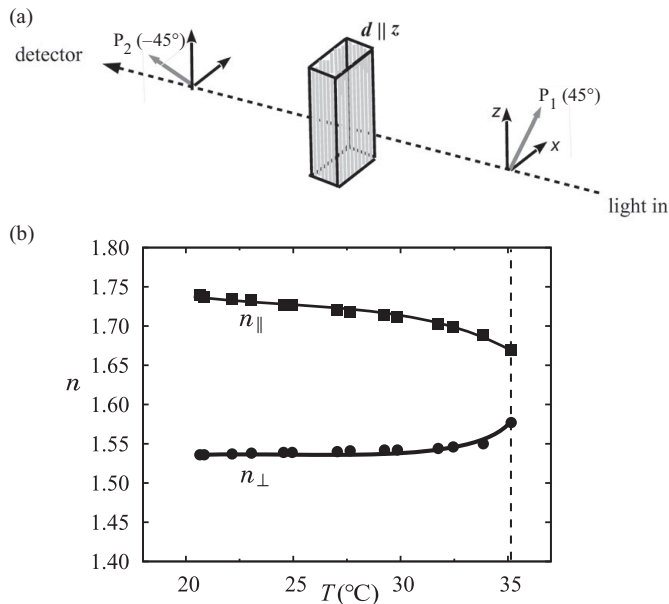


Figure 1.5 (a) Sketch of an experimental setup to measure the birefringence of an aligned nematic from the intensity of light transmitted through the two polarizers P_1 and P_2 at $\pm 45^\circ$ with respect to the director \mathbf{d} . (b) Refractive indices n_{\parallel} and n_{\perp} for the nematic 5CB in the visible ($\lambda = 546.1$ nm) as a function of temperature [Karat and Madhusudana, 1976]. The vertical dashed line indicates the transition to isotropic.

the two crossed polarizers set at $\pm 45^\circ$ from the director of a vertically aligned sample of thickness δ is (see Appendix L)

$$I = I_0 \sin^2(\pi \delta \Delta n / \lambda), \quad (1.5)$$

where I_0 is the input intensity. The birefringence $\Delta n = n_{\parallel} - n_{\perp}$ typically decreases with increasing temperature, as shown in Fig. 1.5b, indicating an increasing disorder in the molecular organization. At a well-defined temperature T_{NI} , the nematic-isotropic transition temperature, the anisotropy vanishes abruptly and the material becomes an ordinary isotropic liquid. We note, however, that even above the transition the isotropic phase has some short-range ordering, with ordered clusters of molecules of a typical size (*coherence length*) ξ_I , that grows larger on approaching the nematic transition from above. This *pretransitional effect* is observed in a relatively large range of temperatures above T_{NI} (some 10–20 degrees) and is demonstrated by the anomalously large susceptibility to an applied electric field (*Kerr effect*) or magnetic field (*Cotton–Mouton effect*) measured, e.g., by the induced birefringence Δn . Thus (see, e.g., [Haynes et al., 2014]),

$$\Delta n = \lambda \mathcal{K} E^2, \quad (1.6)$$

where λ is the wavelength of the probe light, \mathcal{K} is called the Kerr constant and E is the electric field applied. The Kerr susceptibility of nematic liquid crystals is linked to the size of the oriented domains, as we shall see in Section 4.11, and increases on cooling from the isotropic phase, diverging as the temperature approaches a characteristic temperature, T_{NI}^* , which is typically $\approx 1\text{K}$ below the nematic-isotropic transition temperature T_{NI} , as we see in Fig. 1.6, although it can vary for different nematics [Blachnik et al., 2000]. The easy alignment of a nematic when applying an external field is even more strikingly shown by surface alignment. A thin (a few microns thick) nematic film on a glass or polymer slab

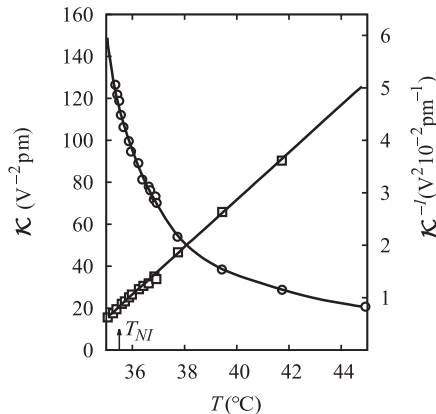


Figure 1.6 Kerr constant \mathcal{K} (○) and its inverse \mathcal{K}^{-1} (□) as a function of temperature for 5CB (obtained from the birefringence Δn at a wavelength $\lambda = 441.6 \text{ nm}$). The divergence temperature $T_{NI}^* = 33.8^\circ \text{C}$ is 1.33 degrees below T_{NI} [Coles and Jennings, 1978]. By comparison, \mathcal{K} of 5CB in a dilute solution of CCl_4 is only $2.8 (\text{V}^{-2} \text{pm})$.

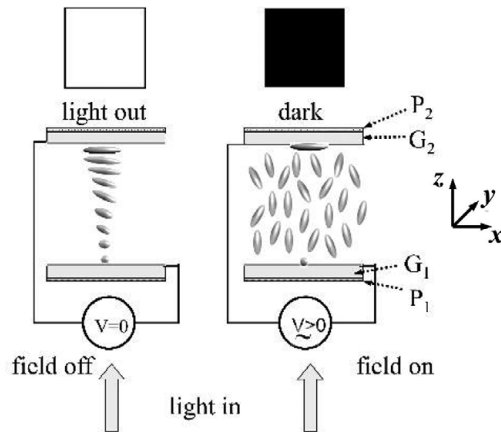


Figure 1.7 Sketch of a twisted nematic (TN) display pixel in electric field off and on states.

can be aligned by surface interactions. An alignment of the director along a certain *easy axis* can be achieved by simply rubbing or lapping the support surface with a soft tissue.

The possibility of changing between the director orientation established by surface forces in a small, micron-size region (a *pixel*) and that obtained by switching on and off an electric field, with the resulting change in the pixel optical properties, is at the heart of the many applications of these mesophases in the electro-optic display industry, where liquid crystal displays (LCDs) have become dominant for applications ranging from mobile phones, TV screens, etc. (see, e.g., [den Boer, 2005; Semenza, 2007; Kim and Song, 2009]). In Fig. 1.7 we see a sketch of the director configurations at rest and with the electric field on for one of the simplest and most widespread LC display types: the twisted nematic (TN). In a TN LCD, a few microns thick film of a nematic with $\Delta\epsilon > 0$ is confined between two glass slides G_1, G_2 , each treated so as to induce a uniform alignment along a certain direction of the surface: $\mathbf{u}_1, \mathbf{u}_2, \mathbf{u}_1 \perp \mathbf{u}_2$. Going across the film from one surface to the other, the director changes in a helical way between the two perpendicular boundary directions. This chiral structure will be able to rotate the plane of the back illumination light, linearly polarized along \mathbf{u}_1 by a first polarizer P_1 , so that at rest (off) light will be able to emerge through the second polarizer, P_2 , set along \mathbf{u}_2 . However, an electric field can be applied to the pixel, printed with a transparent conducting ink (typically, Indium-Tin Oxide, ITO) and connected to the device circuitry. Applying to the pixel a suitable voltage across the two surfaces, the small nematic volume (*voxel*) subjected to the field aligns along the field direction, blocking transmission through the pixel. The pixel then operates as an optical switch: it will appear black when the helix is completely unwound, or partially transparent, according to a number of grey levels n_G (typically $n_G = 256$) established by changing the applied field. When the field is switched off again, the LC interaction with the surfaces will re-establish the original situation of transparency. Colours are obtained by additive synthesis having, instead of a single pixel a set of three (*sub-pixels*) so close that the eye does not spatially resolve them. Illuminating with red, green and blue (RGB) light respectively, n_G^3 colours

can be obtained. Each of the three lights is typically obtained from a white back-light by a colour filter. A more recent and better approach is to illuminate with UV light a film containing semiconductor quantum dots (QDs) [Reed, 1993; Ness and Niehaus, 2011], for instance, CdSe nanoparticles of three different sizes that emit respectively rather pure red, green and blue lights, more easily filtered than the original white light. Even more simply a blue light-emitting diode (LED) can be used to illuminate the polymer film containing two QDs emitting in the red and the green [Luo et al., 2014].

1.2.2 Defects

When a thin film of nematic on an untreated glass slide is observed between crossed polarizers, the birefringence coupled to the distribution of director orientations in the sample yields a typical texture, shown in Fig. 1.8a, called *schlieren* [de Gennes, 1974; Brochard, 1977]. The black threads correspond to regions where the director is in the plane parallel to one of the crossed polarizers or where the system is locally isotropic. The points or lines where these differently oriented directors meet, represent singularities of the director field corresponding to topological *defects* [Frank, 1958; Mermin, 1979; Kleman, 1982; Trebin, 1982; Lavrentovich et al., 2001; Muševič, 2017]. For nematics we note singularities (*noyaux*) with two and four brushes (see Fig. 1.8) that correspond to defects with strength, or *winding number*, $s = \frac{1}{2}$ and $s = 1$, respectively (Fig. 1.8b). The value of the winding number, s , can be assigned, assuming for simplicity that in the thin film the director distribution is two-dimensional, by drawing a closed circuit around the defect and observing the total angle of rotation, α_d , of the director upon returning to the same point. Clearly, α_d is a multiple of π and $s = \alpha_d/(2\pi)$, and the s is just 1/4 of the number of brushes observed. The sign of the defect can be obtained following the movement of the brushes as the polarizers are rotated: the sign is taken to be positive if the brushes rotate in the same direction as that of the crossed polaroids and negative if the brushes rotate in the opposite direction.

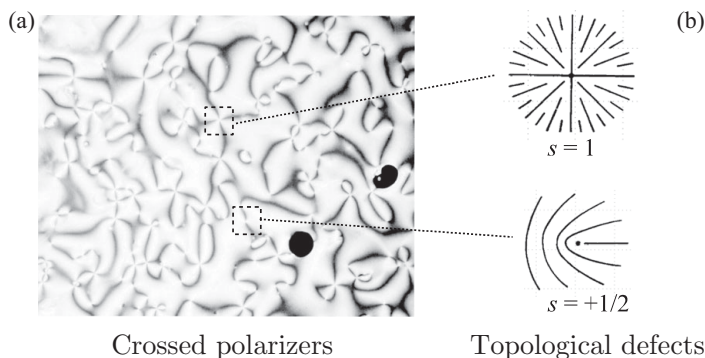


Figure 1.8 The schlieren texture of nematics between (a) crossed polarizers and (b) two topological defects showing the origin of the black threads. The two deep black regions correspond to hotspots, where the nematic has turned isotropic.

The procedure to classify defects can be generalized to director distributions in three dimensions considering a closed sphere surrounding the singular point and applying the methods of algebraic topology, in particular so-called homotopy groups, beyond the scope of this book and well treated elsewhere, e.g. by Kurik and Lavrentovich [1988] and Mermin [1990]. An important point is that, while in two dimensions an infinity of different strengths: $s = \pm 1/2, \pm 1, \pm 3/2, \dots$ can in principle occur, in 3D only defects of strength 1/2 can exist. The polarizing optical microscope (POM) textures of thin films of liquid crystals do not depend on the specific chemical nature of the compound, but, as we shall see, are characteristic, given a certain surface treatment of the film, of the different categories of liquid crystals. Indeed, this constitutes an important practical tool in assigning liquid crystal types [de Gennes, 1974; Gray and Goodby, 1984; Neubert, 2001a].

1.2.3 Elastic Constants

Nematics also present an elastic response: when their director is deformed by applying some weak external field, they return to the original molecular organization as the stimulus is released, somehow similarly to what happens to crystals but not to isotropic liquids [Frank, 1958; Nehring and Saupe, 1971; Stephen and Straley, 1974; Clark, 1976; Crawford and Žumer, 1995; Kleman and Lavrentovich, 2003]. To see how this effect can be observed, let us imagine we align a liquid crystal film with a uniform director in any point of the material and consider this is the state at rest. We can then try to deform the material and write the elastic free energy density \mathcal{G}_{el} for the slightly distorted nematic, following Frank [1958], as an expansion in powers of the (small) gradient components of \mathbf{d} . In the various notations commonly used these are $d_{ij} \equiv \nabla_i d_j \equiv [\nabla \mathbf{d}]_{ij} \equiv [\nabla \otimes \mathbf{d}]_{ij}$. The free energy density can be written as a sum of a bulk term $\mathcal{G}_{\text{el}}^b$, and a surface term $\mathcal{G}_{\text{el}}^s$:

$$\mathcal{G}_{\text{el}} \equiv \mathcal{G}_{\text{el}}(\mathbf{d}, \nabla \mathbf{d}) = \mathcal{G}_{\text{el}}^b + \mathcal{G}_{\text{el}}^s, \quad (1.7)$$

where $\mathcal{G}_{\text{el}}(\mathbf{d}, \nabla \mathbf{d})$ should be invariant for arbitrary sample rotations and changes of sign of \mathbf{d} . Retaining only combinations allowed by symmetry and considering only quadratic terms like in the classical Hooke's law of elasticity gives the classical Frank–Oseen expression [Oseen, 1933; Frank, 1958; Stewart, 2004]:

$$\mathcal{G}_{\text{el}}^b = \frac{K_{11}}{2} (\nabla \cdot \mathbf{d})^2 + \frac{1}{2} K_{22} [\mathbf{d} \cdot (\nabla \times \mathbf{d})]^2 + \frac{1}{2} K_{33} |\mathbf{d} \times (\nabla \times \mathbf{d})|^2. \quad (1.8)$$

The last bulk term can also be written as $+\frac{K_{33}}{2} [\mathbf{d} \cdot (\nabla \mathbf{d})]^2$ and the surface term contains divergence terms [Kleman and Lavrentovich, 2003]:

$$\mathcal{G}_{\text{el}}^s = -K_{24} \nabla \cdot (\mathbf{d} \times \nabla \times \mathbf{d} + \mathbf{d} \nabla \cdot \mathbf{d}) + K_{13} \nabla \cdot (\mathbf{d} \nabla \cdot \mathbf{d}). \quad (1.9)$$

The total elastic free energy is obtained integrating over all the sample volume: $\mathcal{G}_{\text{el}}^{\text{tot}} = \int_V \mathbf{dr} \mathcal{G}_{\text{el}}(\mathbf{d}(\mathbf{r}), \nabla \mathbf{d}(\mathbf{r}))$. We see that the expression for $\mathcal{G}_{\text{el}}^b$ contains only three essential modes of deformation of the director: $(\nabla \cdot \mathbf{d})$, $[\mathbf{d} \cdot (\nabla \times \mathbf{d})]$, $|\mathbf{d} \times (\nabla \times \mathbf{d})|$, called *splay*, *twist* and *bend*, shown in Fig. 1.9. The corresponding *splay*, K_{11} , *twist*, K_{22} , and the *bend*, K_{33} ,

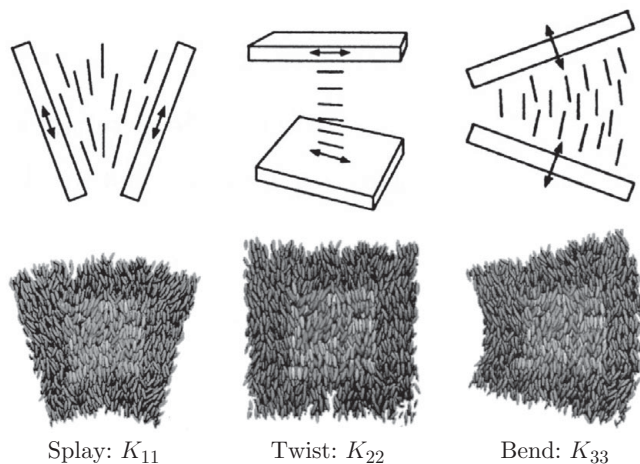


Figure 1.9 A sketch of the splay, twist and bend deformations of a liquid crystal corresponding to the Frank elastic constants K_{11} , K_{22} and K_{33} .

elastic constants [Frank, 1958] express the resistance of the material to these deformations. When calculating the total bulk free energy by volume integration only the first term, \mathcal{G}_{el}^b , survives, while the second, \mathcal{G}_{el}^s , involving the *saddle-splay* constant K_{24} and the mixed *splay-bend* constant K_{13} , averages to 0. However, these contributions should be considered when the system is confined or in any case a surface [Crawford and Žumer, 1995].

The elastic constants (or *moduli*) are positive, different from one another as they correspond to physically different distortions, they change with temperature and pressure and are fairly small, with typical values of the order of piconewtons (see, e.g., Table 1.3). For low-molar-mass nematic liquid crystals the differences between the three elastic constants are normally relatively small [Stannarius, 1998a; Dunmur, 2001] and, accordingly, the approximation of equal elastic constants in nematics is often made in theoretical work. Within this assumption of $K_{11} = K_{22} = K_{33} = K$, $K_{24} = 0$ and the identity Eq. A.27, the integrand becomes the scalar contraction (Eq. A.22) of the director gradient [Ball, 2017]: $\mathcal{G}_{el}^{tot} = \frac{1}{2} K \int_V d\mathbf{r} \|\nabla \mathbf{d}\|^2$. However, it is worth mentioning that in various important cases we may expect the elastic constants to differ significantly. For instance, de Gennes [1977] observed that splay distortions should be unlikely to occur, and, correspondingly, K_{11} should be very large for systems of long rods, like those of polymeric LC (see Section 1.3) because of the crowding of rods at one end caused by splay. This was experimentally observed for a main-chain polyester [Zhengmin and Kleman, 1984] where $K_{11} \approx 0.1 \text{ pN} \approx 10K_{33}$. For another polyester, Martins et al. [1983] found $K_{11} \approx 2 - 3 K_{33}$. In other LC types, like the twist-bend nematic phase found in certain dimers (see Section 1.5), the bend elastic constant K_{33} is much smaller than the other two [Borshch et al., 2013].

In a great variety of instances, the equilibrium distribution of the director can be obtained by setting up and minimizing the elastic free energy subject to appropriate boundary

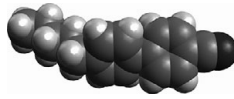


Figure 1.10 A space filling atomistic model of the structure of the nematogen 5CB.

conditions. As discussed by Ericksen [1966], the constants should obey the inequalities [Kleman and Lavrentovich, 2003]:

$$K_{11} \geq 0, K_{22} \geq |K_{24}| \geq 0, K_{33} \geq 0, 2K_{11} - K_{22} - K_{24} \geq 0. \quad (1.10)$$

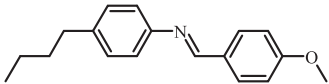
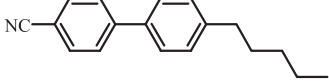
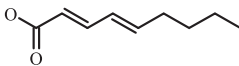
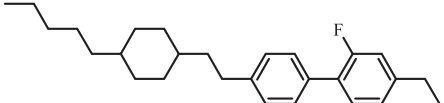
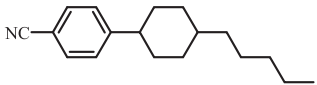
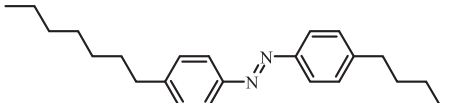
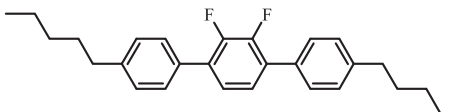
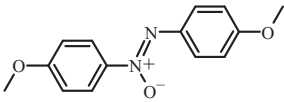
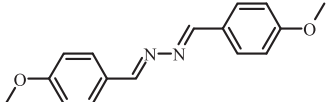
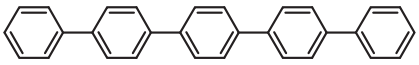
1.2.4 Nematogenic Molecules

Nematics are formed of anisotropic molecules, that is, by molecules, typically non-spherical, which have different properties in different directions. The simplest kind of nematogen molecules, and for a long time the only ones, have elongated (also called *calamitic*) structures. In Fig. 1.10 we show, as an example, the nematogen molecule 5CB. As we can see from a space filling model, where each atom is represented by a sphere of characteristic radius, this molecule is relatively elongated, consisting of a fairly rigid core and of a flexible alkyl chain, although the *aspect ratio* (length to width ratio) is not by itself the only factor determining the existence or absence of a mesophase.

In *thermotropic* materials, nematic phases can be obtained by simply melting a crystal or cooling from an ordinary isotropic phase. In general, the nematicity range is from a few degrees to a few tens of degrees Celsius; then another transition to a solid or to another liquid crystal phase takes place. In Table 1.2 we list the nematic ranges for a few common liquid crystals, taking also the opportunity to introduce their code names. We note that when dealing with nematics we are nearly always in the neighbourhood of a phase transition. In particular, as we see from the data in Table 1.2, the temperature range of nematicity for the pure materials listed here $(T_{KN} - T_{NI})/(273.15 + T_{NI})$ is at most 30% from the nematic-isotropic transition temperature and is not much larger even for mixtures like E63 or Phase 5 especially designed to broaden the interval. The code names in Table 1.2 conform to their common usage and will be used throughout the book. They correspond to the following chemical compositions:

- E63: a commercial mixture (from BDH) of six cyano-biphenyls and terphenyl with a particularly wide nematic range.
- Phase 5: a eutectic mixture with the approximate percent content: 4-butyl, 4'-methoxy azoxybenzene (25 wt%), 4-methoxy, 4'-butyl azoxybenzene (40 wt%), 4-ethyl, 4'-methoxy azoxybenzene (12 wt%) and 4-methoxy, 4'-ethyl azoxybenzene (23 wt%).
- E7: a commercial liquid crystal mixture (from Merck) containing approximately [Lee et al., 2008] 45.53 wt% 5CB, 28.74 wt% 7CB, 16.28 wt% 8OCB ([1,1'-biphenyl], 4-carbonitrile, 4'-octyloxy) and 9.46 wt% 5CT ([1,1',4'-1''-terphenyl], 4-carbonitrile, 4''-pentyl).

Table 1.2. The melting, T_{KN} , and clearing, T_{NI} , temperatures for some mixtures and for pure nematics with their structural chemical formula

Nematic	T_{KN} (°C)	T_{NI} (°C)	Formula
E63	-20.1	87.4	Mixture
Phase 5	-5.1	74.9	Mixture
E7	< -30	58.3	Mixture
E9	6.9	82.4	Mixture
MBBA	20.2	45.9	
5CB	22.5	35.0	
NAD	22.9	48.9	
I52	23.9	103.6	
PCH5	29.9	55.1	
HAB	40.0	47.0	
5FTP	60.0	120.0	
PAA	118.1	135.3	
AAD	168.9	182.9	
P5	400.9	444.9	

- E9: a mixture of 15% 4-propyl, 4'-cyano-biphenyl, 38% 4-pentyl, 4'-cyano-biphenyl, 38% 4-heptyl, 4'-cyano-biphenyl and 9% 4-pentyl, 4'-cyano-terphenyl.
- MBBA: (4-methoxy benzylidene)-4'-n-butylaniline (a Schiff base).
- 5CB: 4-n-pentyl-4'-cyano-biphenyl.

Table 1.3. *Some physical properties of the common nematics PCH5, 5CB and MBBA. PCH5 melts at $T_{KN} = 30^\circ\text{C}$ and becomes isotropic at $T_{NI} = 54.9^\circ\text{C}$, while for 5CB $T_{KN} = 22.5^\circ\text{C}$ and $T_{NI} = 35.0^\circ\text{C}$ and for MBBA $T_{KN} = 22.0^\circ\text{C}$ and $T_{NI} = 48.0^\circ\text{C}$*

Property	PCH5 ^(a) 30.3°C	PCH5 ^(a) 46.7°C	5CB 25.0°C	MBBA 25.0°C
Density, ρ (g cm ⁻³)	0.9630	0.9496	1.022	1.042 ^(d)
Shear (dynamic) viscosity, η (mPa s)	13.96	8.45	28 ^(d)	23 ^(d)
Rotational viscosity, γ_1 (mPa s)	83.2	32.6		
Surface tension, γ (mN/m)			30	
Refractive index, n_{\parallel} at $\lambda = 589$ nm	1.6040	1.5849	1.71 ^(c)	1.764 ^(d)
Refractive index, n_{\perp} at $\lambda = 589$ nm	1.4875	1.4860	1.53 ^(c)	1.549 ^(d)
Dielectric constant, ϵ_{\parallel} at 1 kHz	17.1	15.9	18.5 ^(c)	4.7 ^(f)
Dielectric constant, ϵ_{\perp} at 1 kHz	5.0	5.7	7.0 ^(c)	5.4 ^(f)
Elastic constant, K_{11} (pN)	8.5	5.9	6.2 ^(b)	6.0 ^(f)
Elastic constant, K_{22} (pN)	5.1	3.9	3.9 ^(b)	4.0 ^(f)
Elastic constant, K_{33} (pN)	16.2	9.9	8.2 ^(b)	7.5 ^(f)
Diamagnetic anisotropy, $\Delta\chi$ (10 ⁻⁸ m ³ kg ⁻¹)	3.9	3.7	1.13 ^(e)	9.7 ^(f)

^(a)[Finkenzeller et al., 1989], ^(b)[Dunmur, 2001], ^(c)[Cummins et al., 1975], ^(d, e)[Pestov and Vill, 2005]: ^(d)@ 30°C, ^(e)@ 25.6°C, ^(f)[Priestley et al., 1975].

- NAD: 2,4-nonadienic acid.
- I52: 4-ethyl-2-fluoro-4'-[2-(*trans*-4-*n*-pentyl-cyclohexyl)-ethyl]-biphenyl *n*-propyl-cyclohexyl-ethyl-6-fluoro-*n*-butyl-biphenyl.
- PCH5: 4-*n*-pentyl-4'-cyano-phenylcyclohexyl.
- HAB: 4,4'-diheptyl-azobenzene.
- 5FTP: 4,4''-pentyl-2',3'-difluoro-terphenyl [Gray et al., 1989].
- PAA: 4,4'-dimethoxy-azoxybenzene.
- AAD: anisaldazine.
- P5: *p*-quinquephenyl.

These are just a few common examples of nematics. In Table 1.3 we report, as an example, a few important physical properties for the nematics PCH5, 5CB, and MBBA.

There are now tens of thousands of known compounds giving nematic phases with extremely different chemical structures [Gray, 1962; Demus, 1989; Kaszynski et al., 2001]. In particular, a variety of aromatic, aliphatic, polar and non-polar compounds have been found to yield nematics.

A very interesting class of compounds is also that of mesogens incorporating a metal, or *metallomesogens* (see, e.g., Fig. 1.11), that somehow combine the characteristics of liquid crystals with those of metal coordination complexes [Hudson and Maitlis, 1993; Donnio and Bruce, 1999]. In particular the introduction of metal atoms with a certain hybridization adds enormous possibilities of precisely directing ligands in space, beyond what is allowed by the linear, triangular or tetrahedral geometry of carbon single, double and triple bonds (sp, sp² and sp³ hybridization) with the effect of varying the shape of a mesogen molecule

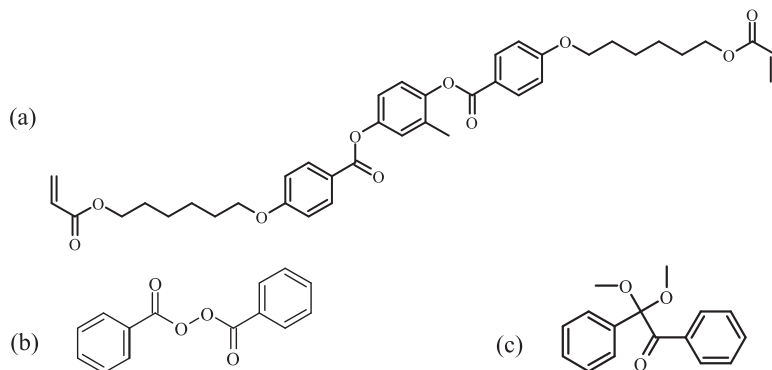
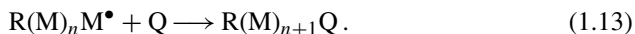


Figure 1.12 (a) A mesogenic monomer: methyl substituted 1,4-phenylene-bis{4-[6-(acryloyloxy) hexyloxy] benzoate} with end reactive acrylates [Broer et al., 1989; Thiem et al., 2005]. On the bottom are (b) the photoinitiators benzoyl peroxide and (c) 2,2-dimethoxy-1,2-diphenylethan-1-one (Irgacure 651[®] from Ciba[®]).

- (ii) Propagation stage. Reaction of the activated species with monomers causes rapid chain growth:



- (iii) Termination step ends the reaction. The polymer chain length grows until, after a certain number of steps, the process is terminated by a quencher species Q which can react with the activated species M[•] but cannot participate in further reactions:



A practical example is that where the monomer M is a reactive mesogen, with two active acrylates groups at the end of the molecule (see Fig. 1.12). The acrylate functional group is particularly reactive, due to the vinyl double bond. Initiation starts by irradiation of the mixture of monomer with photoinitiator (even in very small concentration, $\ll 1\%$) at a wavelength where the host reactive mesogens do not absorb light, so that the photopolymerization can proceed homogeneously through the whole sample. When the active groups are at the end of the elongated monomer, a *main-chain* polymer consisting of a string of monomer units is formed. However, with an alternative strategy mesogenic substituents can be attached to the chain backbone, forming *side-chain* polymers [Finkelmann, 1982; Finkelmann and Rehage, 1984; McArdle, 1989]. In Fig. 1.13 we see schematic examples of main-chain and side-chain polymers [Blumstein, 1978; Finkelmann, 1982; Finkelmann and Rehage, 1984; Samulski, 1985; Gleim and Finkelmann, 1989]. Alignment of LCP chains can be achieved by mechanical stretching of the material in various ways [Xue et al., 2015]. Some interesting classes of composite materials can be obtained performing polymerization of reactive monomers and nematics. Thus, for immiscible liquid crystals (roughly 30%–50%) and partially polymerized but still liquid RMs an emulsion can be formed, which results, by further polymerization (*curing*) of the RMs, in a phase separation producing a dispersion of micron size droplets of LC in a solid polymer. Films of these

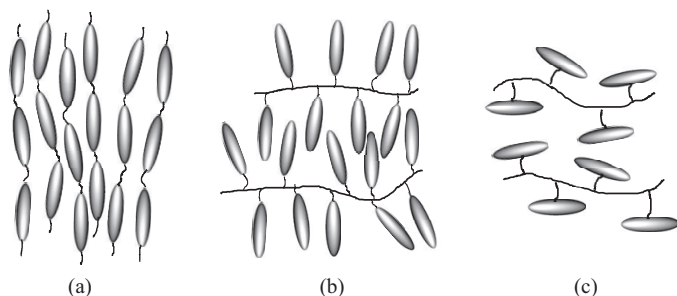


Figure 1.13 Schematics of (a) main-chain, (b) side-chain end-on and (c) side-chain side-on nematic LC polymers showing how monomers are connected to the backbone.

polymer dispersed liquid crystals (PDLCs) [Doane, 1990] scatter visible light giving a non-transparent state that, if the nematic trapped inside the droplets has positive dielectric anisotropy, can be switched to transparent subjecting them to an electric field across the film, with applications, e.g. for smart windows (even if the off opaque state may be non-ideal in many cases).

Increasing the polymer concentration to 60%–80% together with a fast curing with stronger light intensity gives nanosize droplets. A film of such a composite is transparent in the visible, even though it can still be switched, giving fast modulation of light useful in photonics applications. In particular, holographic gratings for switchable transmissive and reflective diffractive optics can be fabricated by the coherent interference of laser radiation of the reactive mixture, hence the name H-PDLC for these materials [Bunning et al., 2000].

A third type of polymer–nematic composites is obtained for low (1%–10%) polymer content, cured in a way that yields a uniform dispersion of the polymer chains (polymer stabilized LC, PSLC) or a polymer network in the nematic. The polymer provides some memory of the original orientation of the polymer chains to the system, facilitating and speeding up switching. A polymer network LC (PNLC) film with *homeotropic* (i.e. perpendicular to the surface) polymer chains orientations loaded with a nematic with negative dielectric anisotropy can be converted from transparent to opaque when a field applied across the film is switched on.

1.4 Chiral Nematics

Chiral¹ nematics, N^* , also called *cholesterics*, are a naturally twisted variety of nematics, where the director assumes a helical configuration. They can be produced by chiral mesogens or by adding a chiral solute to a nematic [Chilaya and Lisetski, 1986; Oswald and Pieranski, 2005], see Fig. 1.14. Curiously, cholesterol esters were the first liquid crystals of any kind discovered (by the botanist Reinitzer in 1888) [Sluckin et al., 2004]. Maybe this is less surprising, when thinking that chiral liquid-crystalline structures abound in plant and

¹ Any geometrical figure, or a group of points or a particle in a d -dimensional space ($d = 1, 2, 3$), is said to be chiral if it cannot be superimposed to its mirror image by any rotation in the same space. The two mirror images or *enantiomers* can be called Left (L) or Right (R).

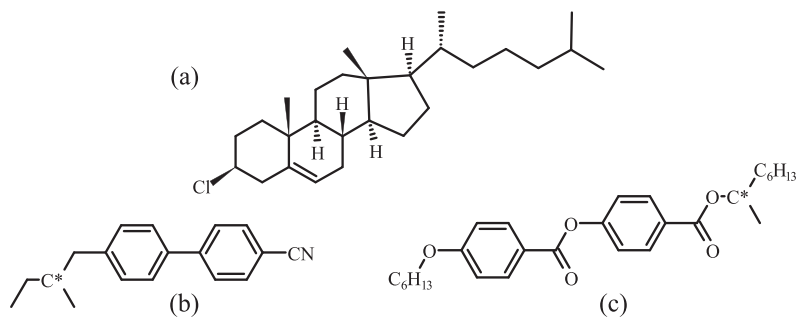


Figure 1.14 A chiral mesogen: (a) cholesterol chloride and two chiral dopants: (b) CB15 and (c) S811 [Ko et al., 2009].

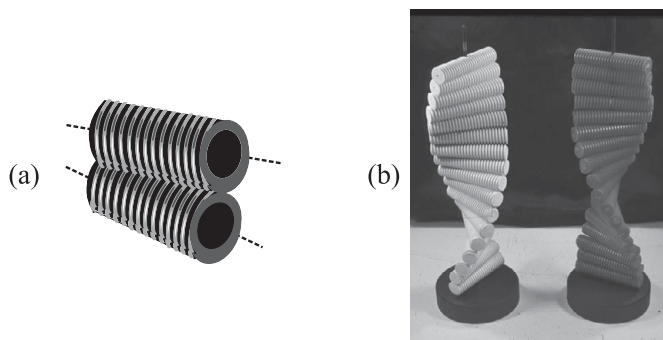


Figure 1.15 (a) Chiral threaded rods in contact cannot be placed exactly parallel to each other, but naturally adopt a twisted mutual orientation when trying to align. (b) They then form a helical organization. Changing the chirality of the rod changes the handedness of the resulting helix.

animal systems [Mitov, 2017]. To see how a chiral mesogen can induce the formation of a twisted structure, a simple hard particle model made of threaded rods can help (Fig. 1.15). The molecular organization in cholesterics is normally represented as in Fig. 1.16, with nematic-like planes twisted one with respect to the next. This model is compatible with the optical properties of cholesterics, but in reality, the system has a uniform distribution of centres of mass, and no true layer structure is present. The repeat distance or *pitch*, p , i.e. the distance over which the local director of the cholesteric helix rotates of 360° , is typically of a few hundred nanometres, so that on a local, molecular scale, very little difference exists between cholesterics and nematics. The environment around a molecule and the ordering of the molecule with respect to the local director is thus quite similar, with the difference that the director remains perpendicular to the helix axis while progressively rotating around it. If the director \mathbf{d} describes a right-handed screw along the laboratory z -axis, in a right-handed coordinate system, its explicit form can be written as:

$$\mathbf{d}(z) = (\cos[q_0 z + \phi], \sin[q_0 z + \phi], 0), \quad (1.14)$$

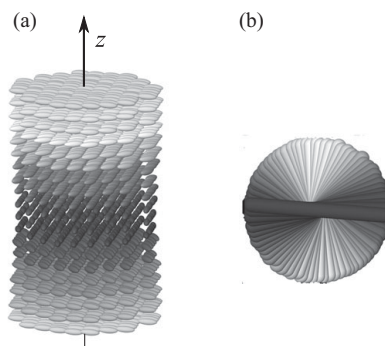


Figure 1.16 A simplified representation of the structure of a cholesteric in terms of nematic regions ('pseudo-layers') (a) twisted one with respect to the other, and (b) a view from top, showing the effective uniaxiality around the helix axis.

where ϕ is an arbitrary phase and $q_0 = 2\pi/p$ corresponds to the repeat distance along the column (pitch) p , with q_0 positive or negative for a right- or left-handed material. The sense of the cholesteric helix is reversed if the chirality of the mesogen is reversed. However, no general way exists of relating the left or right twist of the helix to the absolute conformation or the sign of the optical activity of the mesogen. The fact that chirality is essential to produce optical activity and to give rise to a cholesteric does not mean that the two are directly related but just that they are both not forbidden under the same conditions.

The Frank elastic energy of a chiral nematic, $\mathcal{G}_{\text{el}}^{ch}$, is very similar to the nematic one, but contains the wave vector q_0 :

$$\mathcal{G}_{\text{el}}^{ch} = \frac{K_{11}}{2} (\nabla \cdot \mathbf{d})^2 + \frac{K_{22}}{2} [\mathbf{d} \cdot (\nabla \times \mathbf{d}) + q_0]^2 + \frac{K_{33}}{2} |\mathbf{d} \times (\nabla \times \mathbf{d})|^2. \quad (1.15)$$

The helical structure implies that the plane of polarization of a beam of light propagating along the helix axis will be rotated by an amount proportional to the number of helix windings and thus to the sample thickness in an ideally oriented sample. A one-millimetre-thick sample of uniformly aligned cholesteric can give an optical rotation of the order of 10^4 – 10^5 degrees, a huge amount compared with that caused by single-molecule optical activity or to optical rotation in crystals. By means of comparison, the plane of polarization is rotated by 0.665 degrees upon passing through 1 mm of a water solution containing 10 g/l of sucrose, a simple chiral molecule. The pitch in cholesterics can vary a lot with the nature of the material and for cholesterol esters is in the range 300–500 nm. For a given material the pitch can be easily changed with a variety of perturbation agents: temperature, pressure, impurity concentration, etc.

Cholesteric phases can be also induced by the addition of a small quantity of an anisotropic chiral dopant to a nematic (see Fig. 1.14). The pitch of the induced cholesteric phase, p , is inversely proportional to the chiral dopant concentration C^* , but it is usually longer than that of pure materials, with reflection bands in the infrared (IR) rather than in the visible region. The inverse of the proportionality constant is called *helical twisting power*: $HTP \propto 1/(pC^*)$. The two chiral dopants CB15 and S811 shown in Fig. 1.14(b, c) are an

example of solutes that have large and opposite helical twisting power: $HTP \approx 7 \mu\text{m}^{-1}$ and $HTP \approx -11 \mu\text{m}^{-1}$ respectively, when dissolved in the nematic mixture E7 [Ko et al., 2009].

1.4.1 Selective Wavelength Reflection

It is important to note that the periodic structure of cholesterics can act as a diffraction grid for light with wavelength of the same order of magnitude of its repeat distance. According to classical Bragg law, if we have a beam of white light incident at an angle θ with respect to the helix axis on a transparent cholesteric with an idealized perfectly planar surface, to have constructive interference we need the difference in optical path (the geometric difference of path times the refractive index) to be a multiple of the wavelength $n(\theta)p \sin \theta = m\lambda$, with m an integer, $n(\theta)$ the *effective refractive index* and p being the helix pitch. Assuming nearly normal incidence, $\theta \approx 90^\circ$, this implies selective reflection of light (cf. Fig. 1.17a) at the wavelength $\lambda = p(n_{\parallel} + n_{\perp})/2$ with the bandwidth $\Delta\lambda = p(n_{\parallel} - n_{\perp})$, where n_{\parallel} and n_{\perp} are the extraordinary and ordinary refractive indices of the untwisted liquid crystal. In practice, only the first-order reflection ($m = 1$) appears at normal incidence [Sage, 2011]. At oblique incidence, higher-order reflections can also occur but are generally much weaker. To complicate things further, Bragg's law does not hold exactly when the helix axes are not uniformly aligned, with the incidence angle θ_1 and the observation angle θ_2 that can be different, leading to a more complex expression [Sage, 1992; Yang et al., 1997]. We should also note that the reflected light is circularly or elliptically polarized and has the same handedness as that of the helical structure of the cholesteric phase. A left-handed helix reflects left-handed light, whereas right-handed light passes unaffected (so 50% of the intensity of an unpolarized incident radiation is lost to reflection). Incidentally, this is the opposite of the behaviour of a mirror which reflects circular polarized light with opposite handedness.

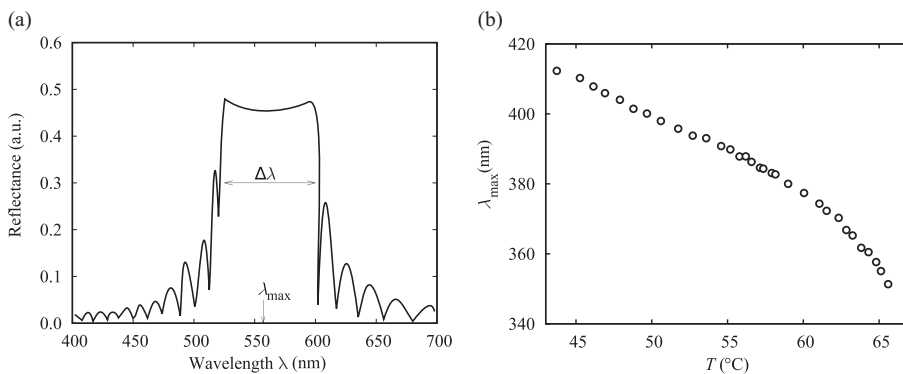


Figure 1.17 (a) Typical spectrum of the reflected light intensity from a cholesteric illuminated with linearly polarized light at normal incidence [Hong et al., 2003] showing the reflection band of width $\Delta\lambda$ centred at λ_{max} . (b) The temperature dependence of the reflected λ_{max} , proportional to the helix pitch, in cholesteryl chloride [Hanson et al., 1977].

A material capable of interacting with light in a well-defined way is called a *photonic material* and in this sense an oriented cholesteric is a one-dimensional (1D) photonic material showing, as described, a band gap around λ_{max} . A more complete treatment for arbitrary incidence can be found [e.g., Dreher et al., 1971; Yang and Wu, 2006]. Thin (5–10 μm thick) cholesteric films with planar alignment of the mesogens at the surface can be prepared (e.g. using a rubbed polyimide alignment layer) yielding a stable planar texture with helices as will be discussed in Section 1.4.2. On a black background, so that the light that is not selectively reflected and is more or less completely absorbed, we can have a reflection colour corresponding to a certain pitch. If we perturb the cholesteric, e.g. by changing temperature, the pitch will also change to a first approximation linearly with temperature and accordingly the reflected colour will change as well. This effect is commonly used to obtain a thermographic map of a surface underlying the cholesteric film. The possibility of easily locating hotspots in a surface has led to applications ranging, e.g. from the non-invasive detection of breast cancer to that of anomalous hot areas in electronic circuits [Sage, 2011]. In most cholesterol derivatives the helix winds itself when temperature increases, with a slow decrease in p on increasing temperature as we see in Fig. 1.17b, typically $dp/dT \approx -0.28\%/^{\circ}\text{C}$ [Pindak and Ho, 1976], while non-steroid chiral nematics usually have $dp/dT \approx 0$ [Chilaya and Lisetski, 1986].

Another fascinating application of cholesterics is in the realization of cavity-less dye lasers. These employ a fluorescent dye dissolved in the cholesteric, e.g. the laser dye 4-(dicyanomethylene)-2-methyl-6-(4-di-methylamino-styryl)-4-H-pyran (DCM), that emits across the reflection band of the host (see Fig. 1.17a). After suitable optical pumping of the dye above a threshold intensity (typically $\approx 10^5 \text{ W/cm}^2$), the fraction of the fluorescent light with emitted wavelength within the transmission bandgap is trapped inside the cholesteric that acts like a cavity resonator. A monochromatic laser light is instead emitted at the band edge (see Fig. 1.18). Note that for a helix with a certain handedness, the light with opposite

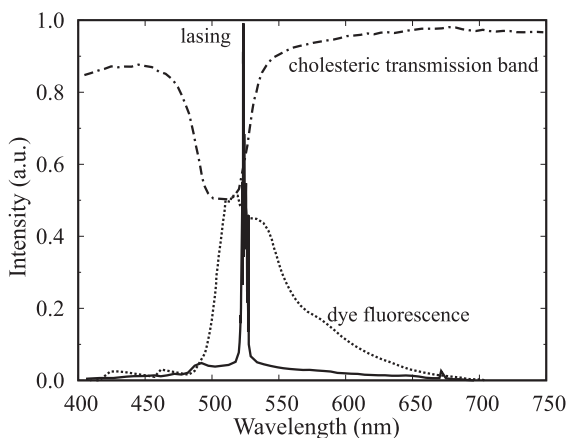


Figure 1.18 An example of cholesteric bandgap (dot-dashed), the emission spectrum of the dissolved dye (dashed) and the laser emission at the transmission band edge (continuous line) [De Santo, 2016].

handedness is unaffected by the structure while that with the same circular polarization shows the band gap. Thus, for instance, for a right-handed helix the emitted light with left circular polarization is transmitted, while the right-handed one is selectively reflected, as discussed before [Chandrasekhar, 1992] and shows lasing. A reason for particular interest in these lasers is that they can be tuned by varying the cholesteric pitch and a number of methods have been used: by the application of an external field to a change of concentration of a chiral agent, etc.

Systems with a cholesteric-like disposition of side mesogenic units have also been prepared [Blumstein, 1978]. It is particularly interesting and somehow surprising that the helical structure of chiral reactive mesogens can be consolidated by polymerization, leading to a well-defined cholesteric pitch, and reflection colour, that will not change with temperature any further.

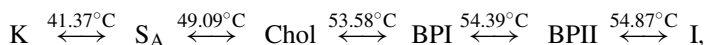
1.4.2 Cholesteric Textures

Chiral nematics exhibit textures at the polarizing microscope that are quite different from those of nematics. The texture of a thin film of cholesterics will depend on the orientations of the mesogens (and then of the helices) with respect to the support surface [Demus et al., 1998]. In Fig. 1.19 we show the main texture types and a sketch of the molecular organizations originating them, well discussed in literature [de Gennes, 1974]. The planar organization selectively reflects incident light as discussed before, while the polydomain one strongly scatters.

A planar configuration realized with a cholesteric film sandwiched between two plates with proper surface treatment can be transformed in a homeotropic one with the helix unwound if the LC has a positive dielectric anisotropy ($\Delta\epsilon > 0$) and a field higher than the critical value $E_c = (\pi^2/p)\sqrt{(K_{22}/(\epsilon_0\Delta\epsilon))}$ is applied [Yang et al., 1997]. Alternatively, applying an intermediate strength field the reflecting planar configuration can be transformed into a strongly scattering focal-conic one where helical domains still exist but are disordered in space. It is interesting to note that both textures, when created, can last without an applied field, providing the basis for a bistable, low power consumption, device. These changes of optical properties, that can be driven pixel by pixel are the basis for a class of cholesteric based reflective LCD [Yang et al., 1997].

1.4.3 Blue Phases

For certain strongly chiral materials, typically among those that have a short pitch, other molecular organizations called *Blue Phases* (BPs) are formed between the cholesteric and the isotropic phase [Crooker, 1983; Kitzerow and Bahr, 2001; Kikuchi, 2008; Rahman et al., 2015]. For instance, cholesteryl oleate has the following sequence of phases, including one of layered smectic phases discussed Section 1.7 [Voets et al., 1989]:



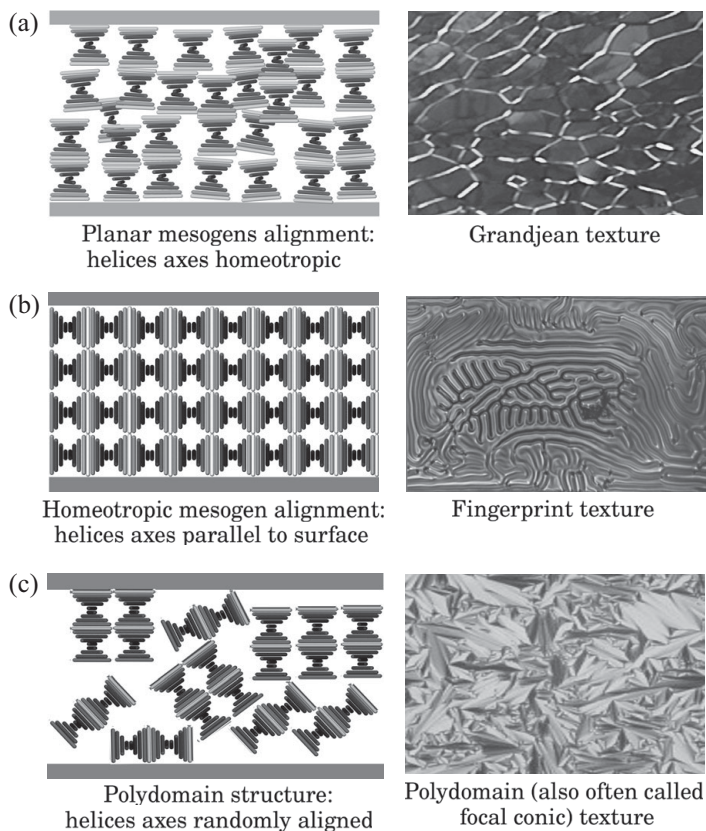


Figure 1.19 Sketches of the arrangement of cholesteric helices in films with different surface alignment (left) and corresponding observed textures between cross polarizers (right). (a) Planar structure with helix axes perpendicular to the support surface. The dark lines in the Grandjean texture (right) are called *oily streaks* [Dierking, 2003]. (b) Helices with local axis parallel to the surface (homeotropic alignment of mesogens) and fingerprint texture [Giordano et al., 1982]. (c) polydomain distribution of helices and real texture [Dierking, 2003].

and cholesteryl nonanoate has three BPs:



These BPs are, differently from cholesterics, optically isotropic: BPI and BP II are cubic, while BP III has spherical symmetry as the isotropic phase [Crooker, 2001] even though they still have large optical activity. The simplest way of visualizing the structure of BPs is probably that of arbitrarily starting from one constituent molecule and a twist propagating from it, not only in a direction perpendicular to its axis, like in a cholesteric, but also in the other perpendicular direction. This structure is called a *double twist cylinder* (see Fig. 1.20). The various phases have complicated superstructures, formed by packing the double twist

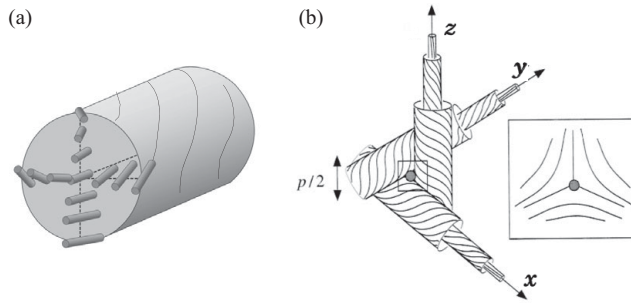


Figure 1.20 (a) Cylindrical structure with twist in two perpendicular directions away from the cylinder axis or *double twist*. The twist increases moving away from the centre of the cylinder and is around 45° at the tube boundary. (b) As three cylinders meet at a corner the directors form a defect [Cao et al., 2002; Kleman and Lavrentovich, 2003].

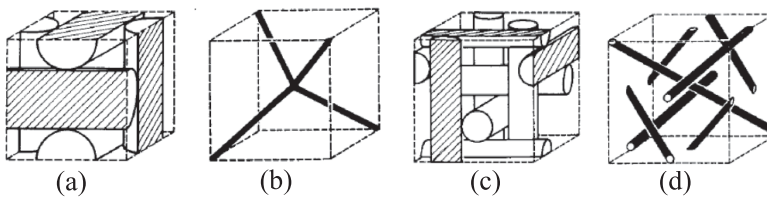


Figure 1.21 The simple cubic (sc) and body centred cubic (bcc) structure of blue phases (a) BPII and (c) BPI and the corresponding unit cells of defect lines (b, d) [Dubois-Violette and Pansu, 1988].

cylinders in various ways. In practice, the unit cells are body-centred cubic for BPI and simple cubic for BPII (Fig. 1.21).

The first BPs only existed in a narrow temperature range and thus were of limited interest for applications, but this has completely changed with the discovery of wide temperature range materials [Coles and Pivnenko, 2005] and of a procedure for stabilizing BPs, widening their temperature range of existence, by the inclusion of suitable polymers, e.g. obtained polymerizing the monomers directly in the BP [Kikuchi et al., 2002]. This stabilization has led to applications in displays, exploiting the very high susceptibility of the BP to an applied electric field: the Kerr effect already discussed (see Eq. 1.6). The field turns the optically isotropic BP into a birefringent medium and opens the possibility of realizing very fast response (<1 ms) displays based on BPs that do not require an aligning film. For instance, while no light would emerge between crossed polarizers at field off, light would be observed as the field is switched on (see Eq. 1.5), even though rather high voltages, of the order of $5 \text{ V}/\mu\text{m}$, some 10 times higher than those of a twisted nematic LCD seen before, are required [Endo et al., 2016].

The periodicity of BPs along different directions is similar to that of cholesterics and also gives the possibility of mirror-less dye lasing, but with emission in three directions rather than in just one as for cholesterics [Cao et al., 2002].

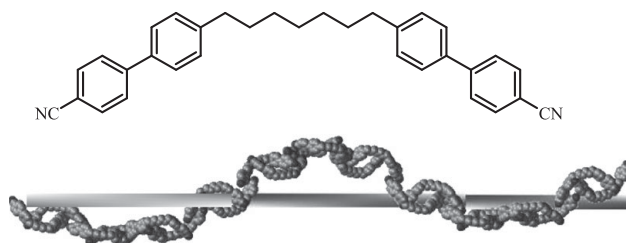


Figure 1.22 A possible model for the twist-bend phase of the cyano-biphenyl dimer CB7CB.

1.5 Twist-Bend Nematic Phase

We have seen how chiral mesogens originate spontaneously twisted nematic (cholesteric) structures with an overall chirality determined by the chirality of the mesogen. More intriguingly twisted nematics have also been predicted in systems of achiral molecules [Dozov, 2001] and observed first in materials containing flexible alkyl spacers with an odd number of CH_2 (methylene) units [Ungar et al., 1992]. In particular, a number of studies have been performed on cyano-biphenyl dimers [Cestari et al., 2011; Borshch et al., 2013; Chen et al., 2013; Zhu et al., 2016] like 4',4'-(heptane-1,7-diyl)-bis([1',1'-biphenyl]-4'-carbo-nitrile) (CB7CB), shown in Fig. 1.22, where the pitch of the structure is found to be around 8 nm using various experimental techniques and in particular soft X-ray resonant scattering at the absorption band edge of the carbon atoms of the molecules [Zhu et al., 2016]. It is amazing that in this phase formed from non-chiral mesogens the pitch is some 50 times shorter than that of typical cholesterics originated from chiral mesogens, as we have seen in Section 1.4. The original prediction was that the twist-bend phase should occur when $K_{33} < 0$ and $K_{11}/K_{22} > 2$ [Dozov, 2001]. Experimentally, these materials have a very low bend elastic constant, with $K_{33} < K_{11}$ [Adlem et al., 2013] but this situation does not seem general or clear [Parthasarathi et al., 2017]. The detailed structure of the twist-bend or heliconical phase N_{TB} , for example, its single or double helical structure, is still an object of much debate [Mandle et al., 2015; Tuchband et al., 2017; Mandle and Goodby, 2018]. In any case, the very short pitch of the structure promises to open the way to various novel applications.

1.6 Biaxial Nematics

The occurrence of nematic phases with biaxial symmetry (N_b), where a second director, corresponding to a preferred orientation of the transversal axis, perpendicular to the first, main one, exists, as shown in Fig. 1.23, has been theoretically predicted for a long time [Freiser, 1970] to occur for mesogens of biaxial, rather than uniaxial, symmetry. However, N_b systems were only relatively recently reported in compounds like *p*-dodecyloxy benzoate diester of 2,5-bis(*p*-hydroxyphenyl)-1,3,4-oxadiazole (ODBP-Ph-OC12) [Acharya et al., 2004; Luckhurst, 2004; Madsen et al., 2004; Merkel et al., 2004; Tschierske and Photinos, 2010] and organo siloxane tetrapodes [Merkel et al., 2004; Figueirinhas et al.,

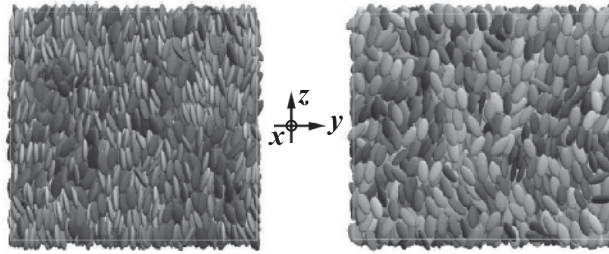


Figure 1.23 Two orthogonal transversal views of a biaxial nematic with the main director along the vertical (z -axis). The difference of the two images shows that molecules tend to stack while maintaining positional disorder [Berardi and Zannoni, 2000].

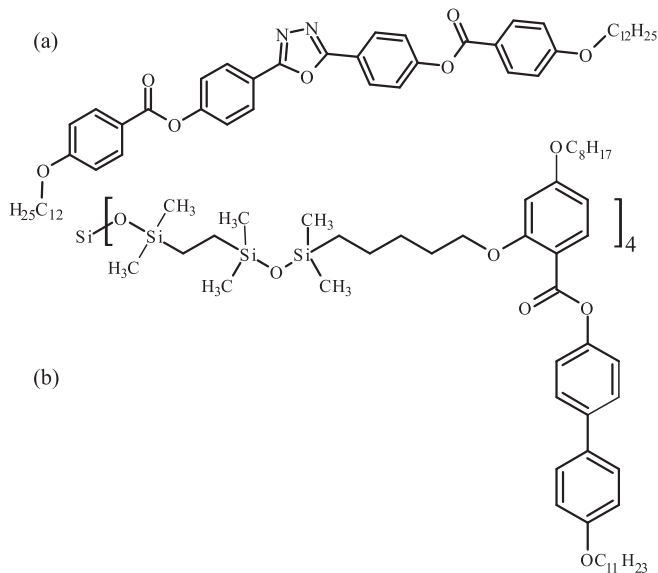


Figure 1.24 Biaxial nematic mesogens: (a) oxadiazole [Acharya et al., 2004; Madsen et al., 2004] and (b) organosiloxane tetrapode [Merkel et al., 2004; Figueirinhas et al., 2005].

2005] (see Fig. 1.24). This may seem strange, since hardly any mesogen is uniaxial, and just looking at molecular shapes they could be better approximated by particles with different thickness in the two directions transversal with respect to the long axis. However, it turns out that the factors favouring biaxial packing also tend to favour biaxial crystal and layered structures, rather than nematic organizations where molecules have to be able to slide one with respect to the other. The observation of a biaxial nematic is thus a difficult compromise to achieve. Biaxial nematics are a matter of active current study both theoretically and experimentally [Luckhurst and Sluckin, 2015]. One of the potential applications explored is the possibility of using an electric field to also control the orientation of the transverse director of a biaxial nematic LC, beyond the only one afforded by the standard uniaxial

materials. In particular, the expectation is that switching this secondary director could be much faster, as also supported by computer simulations [Ricci et al., 2015].

The expression for the elastic free energy for biaxial nematics is much more complex than that for their uniaxial analogue (cf. Eqs. 1.8 and 1.9). The number of invariant terms in an expansion of the free energy to second order of the director derivatives increases to 12 bulk elastic constants and 3 additional surface-like coefficients [Govers and Vertogen, 1984; Stewart, 2015]. Three of the bulk elastic constants describe twist deformations, six of them refer to splay and bend deformations, and the remaining three refer to the coupling of bend and twist deformations.

1.7 Orthogonal Smectics

1.7.1 Smectic A

Smectics [Gray and Goodby, 1984; Oswald and Pieranski, 2006] have a layered structure, as shown in Fig. 1.25, with the mass density not constant as in a uniform fluid, but rather periodic in one dimension. They are thus more ordered than simple nematics and, although still fluids, are more viscous and generally more similar to crystalline phases than nematics and cholesterics. The layered structure corresponds to an ordering in the molecular positions reduced with respect to the three-dimensional one of crystals (cf. Table 1.1). There is a whole family of smectic structures [Goodby and Gray, 1979; Gray and Goodby, 1984; Sackmann, 1989; Goodby and Gray, 1999] corresponding to different molecular organizations within the layer and accordingly to different observable properties. We shall indicate a generic smectic phase with S_m and the various smectic types that we are going to introduce as S_A , S_B , ... with further subscripts or accents as needed to identify subtypes. We describe first the simplest smectic structure, the smectic A (S_A), with molecules perpendicular to the layer and devoid of long-range positional order in the layer itself (Fig. 1.25). In these systems each layer can be thought of, in first approximation, as a two-dimensional liquid, even if it is worth noting that this is somewhat oversimplified. For instance, the molecular mobility along the director, i.e. across the layers, is in many cases actually higher than inside the layers, as found experimentally and with atomistic simulations (see Chapter 12) for 4-*n*-octyl-4'-cyano-biphenyl (8CB). Disrupting the layered structure is an energetically

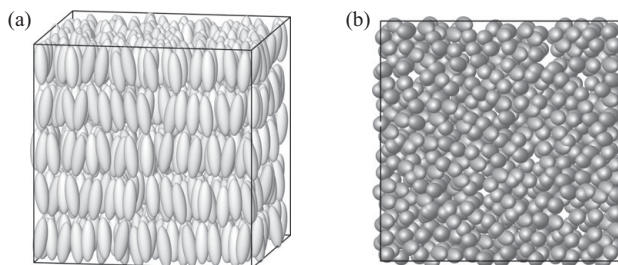


Figure 1.25 (a) The layered structure of a smectic A formed of cylindrically symmetric molecules and (b) a top view showing the fluid-like disorder inside each layer.

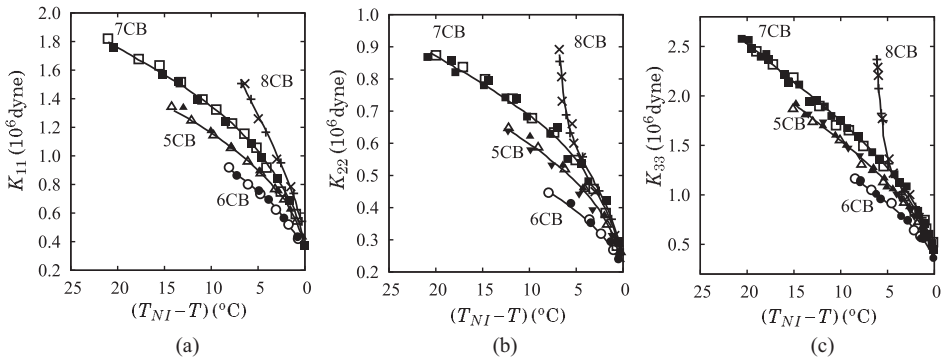


Figure 1.26 Elastic constants of *n*CBs ($n = 5, 6, 7, 8$) as a function of the relative temperature: (a) splay, K_{11} , (b) twist, K_{22} and (c) bend, K_{33} . Results of different experiments are marked separately [Stannarius, 1998b; Pasechnik et al., 2009].

costly process, so of the three Frank deformations seen earlier (Fig. 1.9), only splay (K_{11}) is allowed, while bend and twist are forbidden. Thus, the elastic constants K_{33} and K_{22} related to these deformations will increase and diverge at the transition from nematic to smectic, for a material that presents both phases, for instance 8CB, as shown in Fig. 1.26. In a smectic, the elastic free energy density \mathcal{G}_{el} has to include a term which describes the layer elasticity [Kleman and Lavrentovich, 2003]. In a S_A , we can consider the deformations of a uniform smectic layer with director \mathbf{d} along the layer normal, $\mathbf{d} \parallel \mathbf{z}$ and centred at position $z_0 = z_0(x, y)$ with layer spacing $\ell_{z_0} = \ell_{z_0}(x, y)$. When at rest the layer is flat, so that position z_0 , layer spacing ℓ_{z_0} , and director \mathbf{d} are constant. As the smectic is slightly deformed so that the thickness can vary slightly (by a relative amount $\gamma \equiv (\ell_z - \ell_{z_0})/\ell_{z_0}$) but maintaining the layers parallel and the local director untwisted, we can write [Kleman and Lavrentovich, 2003; Oswald and Pieranski, 2006]

$$\mathcal{G}_{el} = \frac{K_{11}}{2} (\nabla \cdot \mathbf{d})^2 + \frac{B}{2} \gamma^2, \tag{1.16}$$

where B is a Young’s modulus for layers dilation. The preferred organizations are thus those that can be formed without destroying the layers. As an example, we see in Fig. 1.27 a typical smectic A texture at the polarizing microscope, the *focal conic* [Gray and Goodby, 1984], whose origin is strictly linked to the layered organization. In fact, the smectic layers can easily roll and in general take on superstructures that do not involve breaking the layers themselves. In practice, a Swiss roll structure can close in a torus leaving a circular line of discontinuity (or an ellipsoidal one when deformed) as well as a straight line at the joining of the rolls. A particularly interesting way of studying the layered structure of smectics is in films freely suspended across the opening of a thin glass or metal plate, where they form a sort of membrane containing a controlled number of layers (from one or two to thousands). In Table 1.4 we give the transition temperatures for some smectogens. Note that the first one, HAB, is an analogue of the nematic PAA (see Table 1.2), from which it just differs for

Table 1.4. A few smectic A liquid crystals. We report the melting, T_{KA} , the smectic A-nematic, T_{AN} , and the clearing temperature T_{NI} or T_{AI}

Smectogen	T_{KA} (°C)	T_{AN} (°C)	T_{NI} (°C)
4,4'-heptyl azoxybenzene (HAB)	34	54	71
4- <i>n</i> -pentyl-4'-cyano-biphenyl (8CB)	21	32.5	40
Octyloxy-cyano-biphenyl (8OCB)	55	66.7	79.8
Smectogen	T_{KA} (°C)	T_{AI} (°C)	
Diethyl 4,4'-azoxy benzenedicarboxylate	114	122.7	

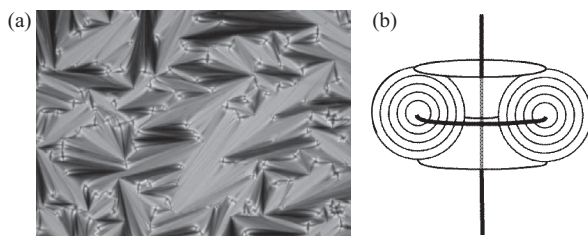


Figure 1.27 (a) The focal-conic fan texture of a smectic A phase observed under the microscope through crossed polarizers and (b) the director tends to lie in the plane of the substrate and the smectic layers are curved across the fans [Dierking, 2003].

a longer alkyl chain. Note also that we can have compounds that go directly from smectic to isotropic phase, as shown in the last entry in Table 1.4.

1.7.2 Strongly Polar Smectics

Only one type of smectic A exists for rod-like, head-tail symmetric, molecules. However, a number of subtypes have been found for smectics formed by asymmetric, polar, molecules, particularly those with strong dipolar end groups and long aromatic cores (see Fig. 1.28). Considering a highly ordered smectic, one has monolayer structures S_{A1} with the polar molecules randomly oriented up and down in the layer and a periodicity similar to the molecular length ℓ_m . Especially with strong terminal dipoles (typically $-\text{CN}$ or $-\text{NO}_2$), bilayer phases S_{A2} with (*antiferroelectric*) ordering of the molecules, up in one layer and down in the next and periodicity similar to $2\ell_m$, are formed. Partial bilayer structures S_{Ad} occur when there is some interdigitation, as we see in Fig. 1.28, with a resulting periodicity ℓ_z intermediate between ℓ_m and $2\ell_m$. For instance, in 8CB $\ell_z \approx 1.4\ell_m$ [Gray and Goodby, 1984]. In both these bilayer phases the dipoles of one layer are schematized as up (down) and their effect is cancelled by those of the adjacent layer. In the *antiphase* smectic A or $S_{\bar{A}}$ there is instead a modulation of dipole orientation inside each layer, with regions of opposite dipoles separated by defect walls which can additionally form a regular stripe or array structure [Levelut et al., 1981; Berardi et al., 1996a]. A change from one type

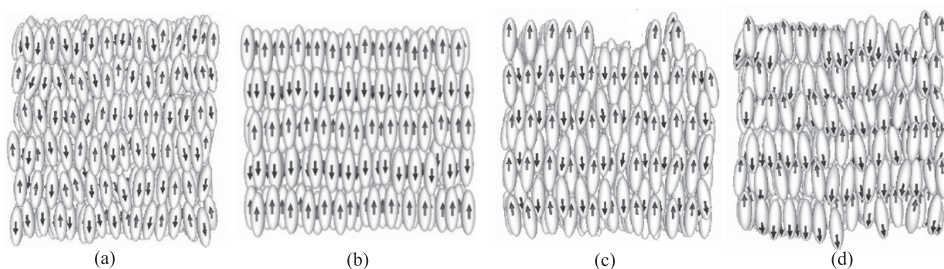
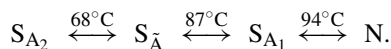


Figure 1.28 Schematic organization of mesogens with a strong axial dipole (black arrow) in smectic A phases showing (a) monolayers in S_{A1} , (b) bilayers in S_{A2} , (c) interdigitated structures in S_{Ad} and (d) alternating stripes of up and down dipoles in S_{A-} [Berardi et al., 2002].

of organization to another can occur with temperature. For instance, in *p*-heptylphenyl-*p*'-nitrobenzoyloxybenzoate (DB_7NO_2) we have the sequence



The behaviour is also observed in mixtures, e.g. of pentylphenyl cyanobenzoyloxy benzoate (DB_5CN) and cyanobenzoyloxy pentyl stilbene (C5 stilbene) [Young et al., 1994]. It is interesting that in some of these strongly associated systems, after cooling from nematic to smectic, a new, *re-entrant*, nematic is obtained upon further cooling (see, for instance, Chapter 2). The different types of pairing lead to different effective repeat units and correspondingly to different X-ray patterns (cf. [Ostrovskii, 1993] and references therein). The possibility of positional order within the layers opens the way to a number of smectic phases [Collings, 1990]. Here we see only a few important ones.

1.7.3 Twist Grain Boundary Smectics

When a cholesteric also has a smectic A, e.g. for cholesteryl nonanoate and decanoate, the pitch diverges at the smectic transition temperature T_{AN} . A typical temperature dependence is [Pindak et al., 1974; Pindak and Ho, 1976]

$$p(T) = p_0 + a(T - T_{AN})^{-\nu}, \quad (1.17)$$

where p_0 is the pitch far away from the smectic transition and ν is a critical exponent (see Chapter 2). For cholesteryl nonanoate and decanoate $\nu \approx 0.66$, similar to theoretical predictions, but other values have been found in different materials [Chilaya and Lisetski, 1986]. In the smectic A phase formed of chiral molecules or S_{A-}^* , Renn and Lubensky [1988] have predicted and Goodby et al. [1989] have observed a helical phase constituted of smectic slabs of a certain thickness ℓ_b (≈ 20 nm) separated by surfaces containing regularly spaced screw dislocations or twist grain boundaries. This phase that has on the one hand

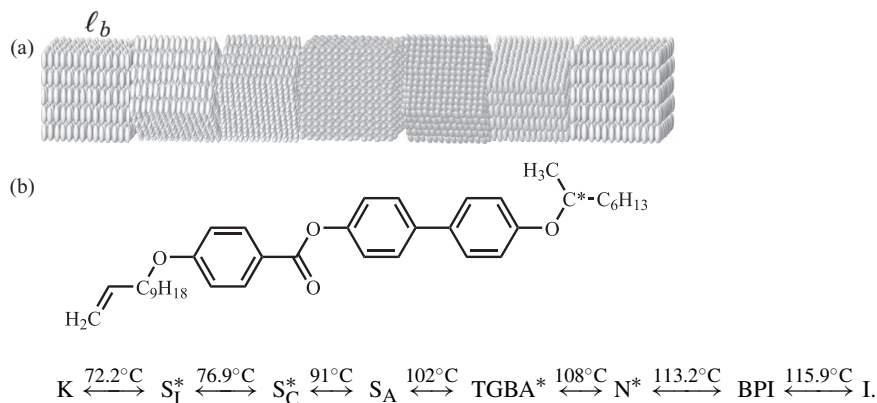


Figure 1.29 (a) A schematic representation of the TGB smectic phase, showing the twisting of S_A slabs of typical thickness ℓ_b [Zhang et al., 2006a]. (b) The chiral compound 4-[4'-(1-methyl heptyloxy)] biphenyl-4-(10-undecenyloxy) benzoate (11EB1M7) and its phase transitions. The S_I^* and S_C^* are chiral versions of the tilted smectics of Fig. 1.32.

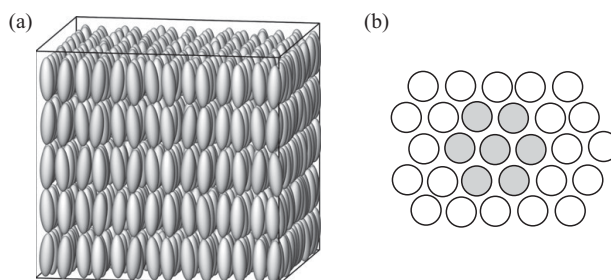


Figure 1.30 (a) The layered structure of a smectic B and (b) a sketch of its local hexagonal clustering.

smectic planes and on the other an average director twist is called *twist grain boundary* (TGB or TGBA*) (see Fig. 1.29).

1.7.4 Smectic B

Smectic B (S_B) systems have a layered structure with molecules perpendicular, on average, to the layer normal and are therefore superficially similar to smectic A (cf. Fig. 1.30a). However, they have a higher viscosity than smectic A and, differently from them, here we have some hexagonal clustering of the molecular centres, as schematically represented in Fig. 1.30b. This kind of ordering is called *bond order* (see Section 4.9.2) and the smectic B phase can be considered as a bond-orientationally ordered version of a smectic A [Brock et al., 1989]. The clusters of hexagonally ordered molecules can themselves be orientationally ordered or disordered with respect to one another. In this last case the

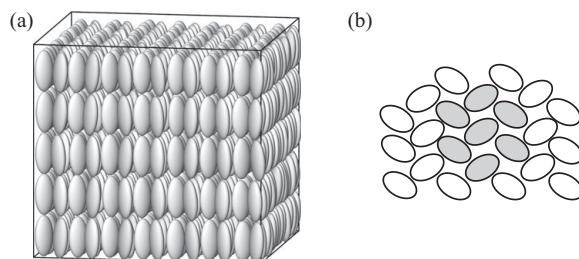
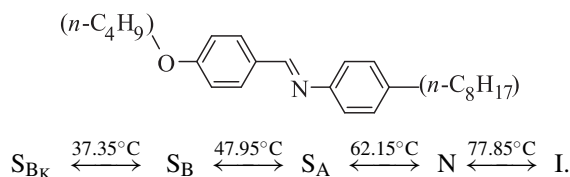


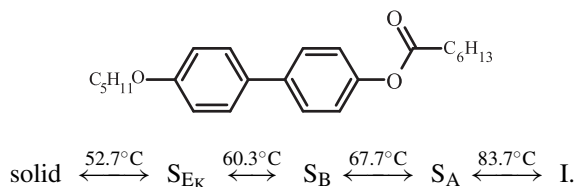
Figure 1.31 (a) The structure of a smectic E and (b) a sketch of the herringbone arrangement of the short molecular axes of its mesogens.

structure of what is called a crystal smectic B (S_{BK}), to distinguish it from the locally hexatic (S_B) one, is really very similar to a true crystal. An example of a molecule giving smectic B phases is: 4'-*n*-butyloxy benzylidene-4-*n*-octylaniline (4O.8) [Birgeneau et al., 1981; Pershan et al., 1981; Gray and Goodby, 1984] which has the sequence [Juszynska et al., 2011]:



1.7.5 Smectic E

In describing the smectic B phase, we have focussed on the layer structure, with molecules essentially orthogonal to the layer, and on the fact that the centres have a hexagonal order, more or less correlated. In reality we should consider also the fact that the molecules are not cylindrically symmetric and that the short axes can have a preferred orientation too. Indeed, while in the smectic B phase the short axes are disposed in a way that preserves a macroscopic uniaxial symmetry, in the smectic E phase, which is very similar to the smectic B, we have instead a herringbone arrangement of the short axes (cf. Fig. 1.31b) and the resulting mesophase is biaxial. As for the S_B , we can have a more crystal like variety, S_{EK} . An example of a compound having a smectic B and a crystal E phase is *n*-hexyl-4'-*n*-pentyloxy biphenyl-4-carboxylate (65OBC). This has a two-dimensional hexatic structure and transitions [Van Roie et al., 2005]:



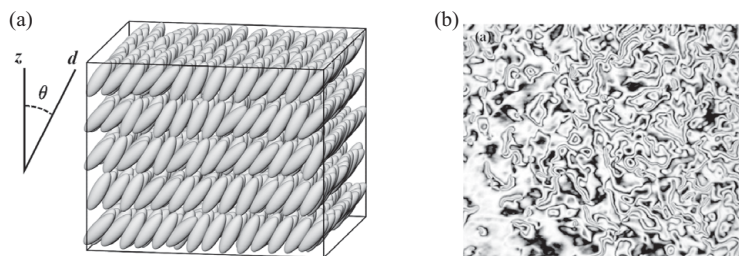


Figure 1.32 (a) Molecular organization in a monoclinic S_C phase and (b) schlieren texture of a smectic C [Sepelj et al., 2007].

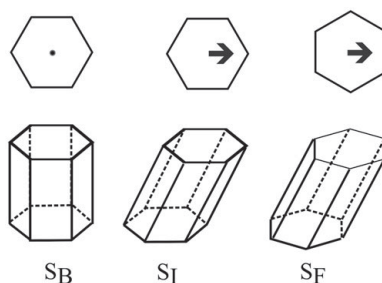


Figure 1.33 A scheme of the various smectic phases with local hexagonal order: the orthogonal smectic B and the tilted smectic I and F.

1.8 Tilted Smectics

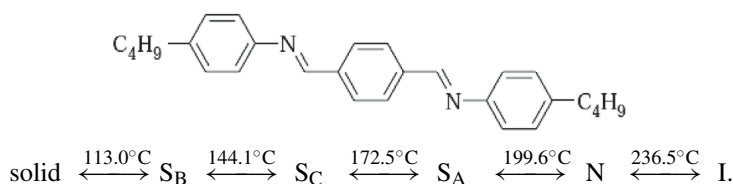
1.8.1 Smectic C

The smectic C phase corresponds to a tilted version of a smectic A, as sketched in Fig. 1.32a, without long range positional ordering inside the layers. However, there exist tilted versions of the upright monolayer, S_{A1} , and bilayer, S_{A2} , phases discussed in Section 1.7.2, i.e. the S_{C1} and S_{C2} . In the same way there exist tilted versions of the smectic B phase. These can be further distinguished by the direction of the tilt with respect to the hexagonal neighbour structure, as can be seen in the summary Fig. 1.33. Thus, S_I and S_F are tilted S_B with inclination direction pointing towards a vertex of the hexagonal cluster of nearest neighbours or perpendicular to a hexagon side. As for the S_B , this positional hexagonal order is only local, if instead it has a long-range character, the S_J , S_G phases, the analogous versions of the crystal S_B are obtained. Yet another version, the smectic L (S_L), with tilt direction intermediate between that shown in Fig. 1.33 for S_I and S_F has been proposed [Chaikin and Lubensky, 1995] and found in some experiments [Chao et al., 1998]. The director \mathbf{d} makes an angle, called the *tilt angle* θ , with the layer normal, which can vary with temperature in some materials, e.g. in terephthalidene-bis-(4-*n*-butylaniline) (for short TBBA) while it is temperature independent in others, like 4,4'-di-*n*-heptyloxyazoxybenzene (HAB). For materials that present both a S_A and a S_C phase, the layer spacing normally shrinks going from S_A to S_C and this corresponds to the simple idea of a rigid molecule

Table 1.5. The melting, T_{KC} , smectic C-nematic, T_{CN} , and nematic-isotropic, T_{NI} , transition temperatures for a few smectic Cs

Smectogen	T_{KC} (°C)	T_{CN} (°C)	T_{NI} (°C)
4,4'-heptyloxyazoxybenzene (HAB)	74	94	124
4,4'-octyloxyazoxybenzene (OAB)	80	108	126
4-octyloxy benzoic acid (OOBA)	101	108	145

tilting away from the normal of a tilt angle. However, this is not the case in the so-called DeVries smectics, that have recently attracted much interest. A possible explanation is that for these systems the molecules are distributed in a kind of conical (and thus uniaxial) way around the layer normal (see [Lagerwall and Giesselmann, 2006; Gorkunov et al., 2007]) even in the S_A phase. It is worth pointing out that some materials exhibit a rich LC polymorphism. For instance, TBBA shows the following cascade of phases [Doucet et al., 1973]:



In Table 1.5 we give the temperature of transition for some common smectic C materials. An ordered smectic C has a C_{2h} symmetry, with the twofold axis perpendicular to the director and in the layer plane. The presence of the inversion centre is not compatible with a macroscopic polarization, which is a vector. The optical properties of a smectic C are similar to those of a biaxial crystal. A polarizing microscope texture of this phase is shown in Fig. 1.32b. Note the nematic-like aspect but with four streak-only centres. For polar smectogens monolayer, partial bilayer and bilayer smectic C phases can exist as for smectic A.

1.8.2 Chiral Smectic C

When the smectogen molecules are chiral or when a chiral solute is added to a smectic C, a phase with macroscopically helical symmetry called *chiral smectic C* or S_C^* can be generated. A centre of symmetry cannot exist any more and the symmetry of the phase is reduced from C_{2h} to C_2 . If we visualize the director in a smectic layer as tilted, we can think that its tip rotates as we move through the layers (see Fig. 1.34), thus generating a helix of given pitch. If the molecules possess a transverse dipole the projection of the dipole in the layer plane is randomly distributed in the layer plane itself and thus there is no resulting net dipole. However, the dipoles can be easily oriented by applying an electric field along a direction parallel to the layer planes. The basic constraint of preserving the tilted structure can then be maintained with the macroscopic polarization along the C_2 axis.

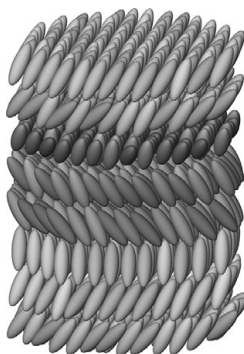
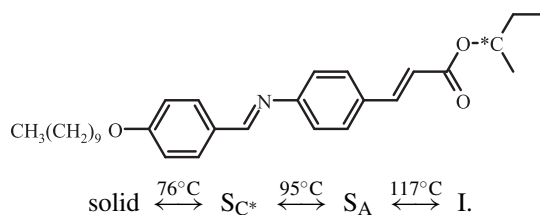
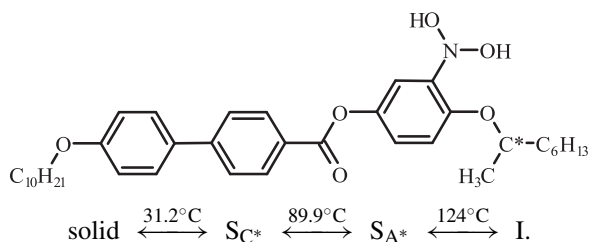


Figure 1.34 A sketch of the smectic C* molecular organization showing the tilted layers twisting along the layer normal.

The system is ferroelectric and is the basis for certain electro-optic displays [Gray, 1987]. An example of compound of this kind is (S)-4-*n*-decyloxy benzylidene amino-2'-methyl butyl cinnamate (DOBAMBC):



Another compound is (S)-4'-(decyloxy)-4-[(1-methylheptyl)oxy]-2-nitro phenyl-[1,1'-biphenyl]-4-carboxylic acid ester (W314) [Jang et al., 2001]



1.8.3 Banana Phases

Ferroelectric S_{C^*} phases are formed by chiral mesogens, so that the discovery [Niori et al., 1996] that ferroelectric phases could be formed by non-chiral mesogens, with an unusual banana, rather than rod-like, shape (see Fig. 1.35) was particularly striking [Jákli et al., 2018]. Excluding a molecular chirality of some conformations, allowed by internal flexibility, a helical S_{C^*} structure can ensue from the supramolecular chirality of the smectic layers with tilted bow molecules endowed with a transversal dipole moment (see Fig.

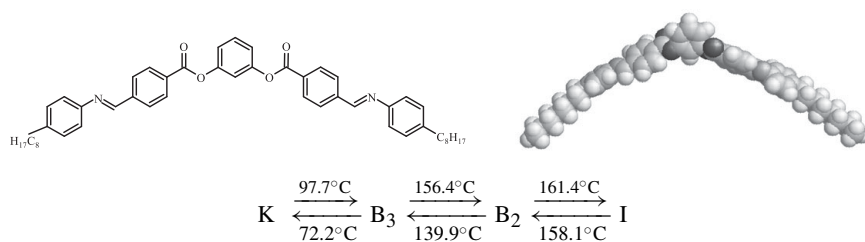


Figure 1.35 Chemical structure and atomistic model of a bent shape mesogen exhibiting tilted smectic ('banana') mesophases (B_2 , B_3) together with its transition temperatures [Niori et al., 1996; Pelzl et al., 1999].

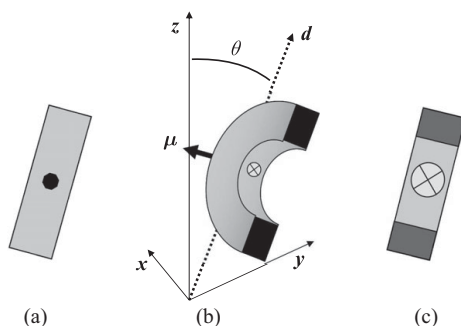


Figure 1.36 Chirality resulting from tilted bent shape mesogens belonging to a smectic layer. The dipole moment μ is transversal to the bow. (b) A sketch of the banana molecule and of (a) a view from the front and (c) back sides.

1.36). The stack of layers can tilt in the same direction (*sinclonic*) or in opposite directions (*anticlionic*) with respect to the layer normal (see Fig. 1.37). Successive smectic layers can be either ferroelectric (with the same direction of polar order) or antiferroelectric (with opposite directions). It is worth noting that the packing of the banana molecules leads to smectic rather than nematic phases, even though nematic phases have been found, e.g. from 4-cyanoresorcinol with short terminal alkyl chains [Keith et al., 2010]. Indeed, a variety of smectic organizations has been found [Link et al., 1997; Pelzl et al., 1999; Coleman et al., 2003] and a specific nomenclature: B_1 , B_2 , ..., B_7 was suggested, with the subscript n corresponding to a conventional indexing of the different phases. This can be a bit confusing, since the phases are rather different and not smectic B after all, and a more recent approach to nomenclature has been based on the arrangement of layers and of layer polarity leading to ferroelectricity or antiferroelectricity (see Fig. 1.37). A detailed treatment of the classification is reported in the reviews by Reddy and Tschierske [2006] and Jáklí et al. [2018]. As for the rather complex physical properties features of the various phases, these are definitely beyond the aims of this book, and we just refer to specific treatments, like those found in [Pelzl et al., 1999; Coleman et al., 2003; Reddy and Tschierske, 2006; Jáklí et al., 2007; Takezoe and Eremin, 2017; Jáklí et al., 2018].

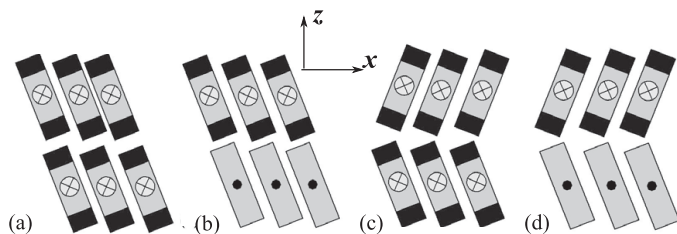


Figure 1.37 A sketch of the molecular organizations that can be obtained in two contiguous layers of banana molecules: (a) sinclinc ferroelectric (SC_{SPF}); (b) sinclinc antiferroelectric (SC_{SPA}); (c) anticlinic ferroelectric (SC_{APF}); (d) anticlinic antiferroelectric (SC_{APA}). The z -direction is along the smectic layer normal.

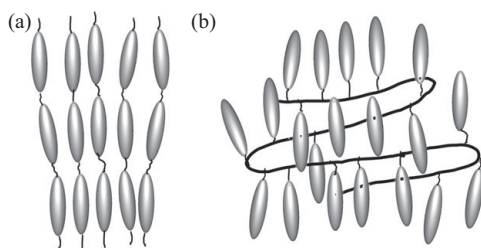


Figure 1.38 A sketch of (a) a main-chain and (b) a side-chain smectic LC polymer.

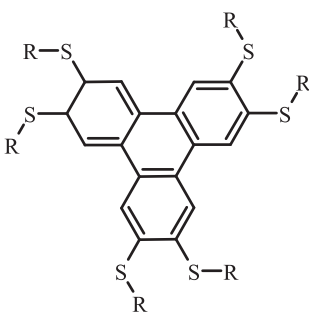
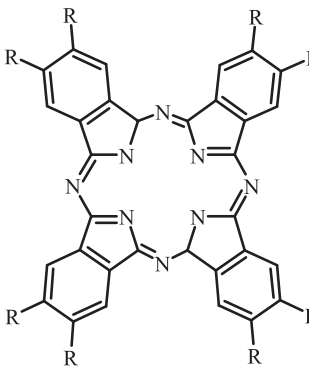
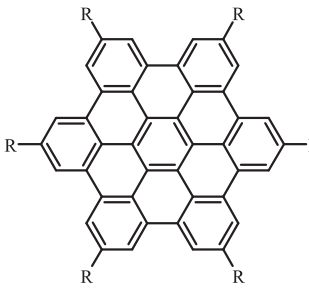
1.9 Smectic Liquid Crystal Polymers

Besides a nematic organization of the side chains in a linear polymer like that in Fig. 1.13, a smectic organization can also exist. Various other types of low-molar-mass liquid crystals presented earlier on have analogues in the polymer field. Here we see, in Fig. 1.38, a sketch of the structure of a smectic main-chain and side-chain polymer where strong lateral interactions of the monomers lead to layered organizations.

1.10 Discotic and Columnar Phases

Disc-like molecules can organize themselves, face parallel, and produce a variety of *discotic* phases [Chandrasekhar, 1982; Guillon, 1999; Bushby and Lozman, 2002; Kumar, 2002; Sergejev et al., 2007; Bisoyi and Kumar, 2010; Wohrle et al., 2016; Gowda and Kumar, 2018]. The basic unit is typically a disc or board shape core with flexible chain substituents as, for example, in hexa-*n*-alkanoates of benzene and triphenylene or in a variety of phthalocyanines, both with and without central metal, or condensed aromatics, like hexabenzocoronene (see Table 1.6). Thus, we can have discotic nematics [Praefcke, 2001] formed by single mesogens, N_D , or by short columnar stacks N_C (see Fig. 1.39) or the chiral variety, nematic N_D^* , i.e. discotic cholesteric. Although nematic discotics N_D do exist, their occurrence is quite rare and more often the molecules organize in long columnar aggregates [Chandrasekhar, 1988] (cf. Fig. 1.40) and actually in the large majority of cases the transition is directly from the isotropic to a columnar phase. The discotic phases can

Table 1.6. Some discotic molecules and their phase transitions (see text and Figs. 1.40 and 1.42)

Molecule	Chemical structure
(a) HHTT R = C ₆ H ₁₃	[Fontes et al., 1988]
$K \xrightarrow{62^\circ\text{C}} D_h^h \xrightleftharpoons{70^\circ\text{C}} D_h^d \xrightarrow{93^\circ\text{C}} I$	
(b) Phthalocyanine R = CH ₂ OC ₁₂ H ₂₅	[Sergeyev et al., 2007]
$K \xrightarrow{79^\circ\text{C}} D \xrightarrow{185^\circ\text{C}} D_h \xrightarrow{260^\circ\text{C}} I$	
(c) Hexabenzocoronene: HBC-(C ₁₄) ₆ R = C ₁₄ H ₂₉	[Pisula et al., 2005]
$K \xrightleftharpoons{114^\circ\text{C}} D_h^o \xrightleftharpoons{\approx 420^\circ\text{C}} I$	

of course be polymerized, like we have seen for rod-like nematics, and in Fig. 1.41 we see an example of a discotic nematogen that can be made reactive by introducing acrylate end groups. There can be various kinds of columnar organizations, usually labelled generically D (or Col by other authors) phases [Luz et al., 1985] if additional details about the

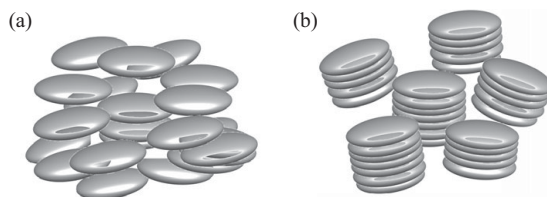


Figure 1.39 Schematic organization of (a) a nematic discotic, N_D and of (b) a columnar nematic, N_C .

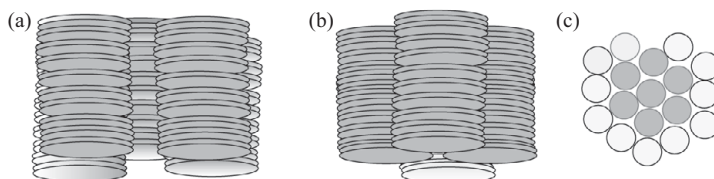


Figure 1.40 Uniaxial columnar liquid crystals with (a) molecular disorder (D_h^d) or (b) some positional order (D_h^o) inside the disc stacks and (c) hexagonal arrangement of the columns.

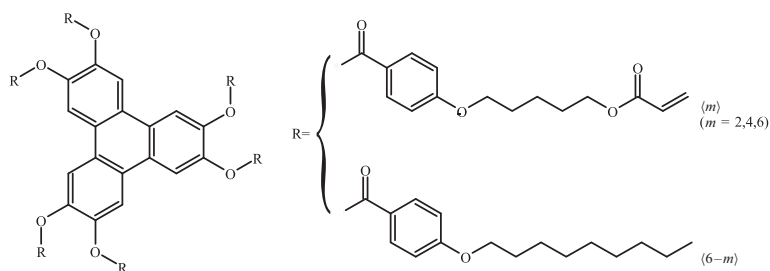


Figure 1.41 A reactive discotic nematogen consisting of a triphenylene core with a total of six alkoxybenzoate substituents (R), of which an average number $\langle m \rangle$, with $\langle m \rangle = 2, 4$ or 6 have reactive acrylate end groups (top right ones) and the remaining $\langle 6 - m \rangle$ are devoid of polymerizable acrylate and thus inactive [Kim et al., 2017].

structure are not available. More specific features of the arrangement inside the columns are indicated with superscripts, with the organization of the columns themselves indicated by subscripts. Thus, if the discs belonging to a column are not regularly positioned, so that we have one-dimensional disorder along the columns the further superscript d is added. If the discs are instead ordered inside the columns, a superscript o , or h if the order is helicoidal (like in the case of HHTT), is employed. A tilt of the mesogens with respect to the column axis is indicated by a superscript t .

The columns themselves can form a more or less regular two-dimensional (2D) array, corresponding to a 2D positional order of the columns, that is manifested with a subscript (h for hexagonal, r for rectangular, ...) as well as orientational order of the molecules. In Fig. 1.40 we see hexagonal, uniaxial phases with or without order inside the column: D_h^o

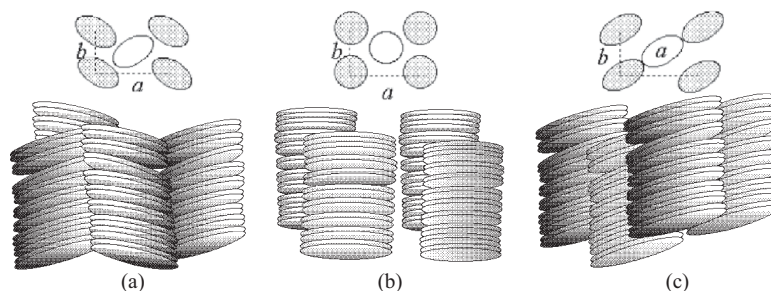


Figure 1.42 Liquid crystals with (a) a tilted arrangement of the columns and (b) a column arrangement which is on average upright, D_r^{dt} , D_r^d (see text) or (c) oblique disordered columns, D_{rt}^d .

and D_h^d . In the absence of further subscripts the columns are assumed to be upright with respect to a hypothetical support surface, while an oblique arrangement of the column axis is marked by a subscript t. Note that, even if chains attached to the periphery of the molecules are not explicitly shown, they play an important role in stabilization. Symmetric substituted discotics tend to give a hexagonal column arrangement and typically give a planar alignment of the discs, i.e. homeotropic alignment of the columns when deposited on a planar surface. Unsymmetrical discotic molecules tend to give tilted phases with rectangular columnar 2D arrangements and their surface alignment is typically non-homeotropic but side on, with the column axes parallel to the surface. Having said that, systems like some substituted phthalocyanines can change morphology with a change of temperature. We also see in Fig. 1.42 various (upright D_r^d , D_r^{dt} or oblique D_{rt}^d) biaxial phases with a rectangular 2D lattice of the columns. The organization shown for the D_r^{dt} phase corresponds to the model proposed by Goldfarb et al. [1983a] in their studies of truxene-hexalkanoate derivatives, with the molecules tilted with respect to the column axis in opposite (anticlinic) directions in alternating columns. The macroscopic symmetry of the D_r^{dt} phase is in any case orthorhombic, while that of the D_t phase is monoclinic. While columnar mesophases are easily found, N_D are available (see Table 1.7) but much more rare [Gasparoux, 1980; Praefcke, 2001; Bisoyi and Kumar, 2010]. The presence of substituents with large steric hindrance seems important in producing the discotic nematic as well as or instead of the stacked, columnar mesophases. Note that in a N_D phase the molecule symmetry axis is on average aligned with respect to the director, like in a normal calamitic nematic. However, the anisotropy in molecular properties with values larger in the plane of the rings (e.g. the polarizability for an aromatic core) tends to be negative rather than positive. Yet another possibility is that the columns themselves form a nematic phase, called a *columnar nematic* N_C . These thermotropic systems have been prepared from a mixture of strong electron donor disc molecules (superdiscs) with small electron acceptor molecules that very efficiently pack in columns [Praefcke et al., 1992]. Examples of superdiscs include pentakis (phenyl ethynyl) phenyl derivatives, while electron acceptor dopants include 2,4,7 trifluorenone. It

Table 1.7. The crystal-columnar, T_{KD} , columnar-nematic, T_{DND} , and nematic-isotropic, T_{NDI} , transition temperatures for a few hexa-R-benzoate triphenylene discotics [Gasparoux, 1980]

R substituent	$T_{KD}(^{\circ}\text{C})$	$T_{DND}(^{\circ}\text{C})$	$T_{NDI}(^{\circ}\text{C})$
$\text{C}_6\text{H}_{13}\text{O}$	186	193	274
$\text{C}_9\text{H}_{19}\text{O}$	154	183	227
$\text{C}_{10}\text{H}_{21}\text{O}$	142	191	212
$\text{C}_{11}\text{H}_{23}\text{O}$	145	179	185

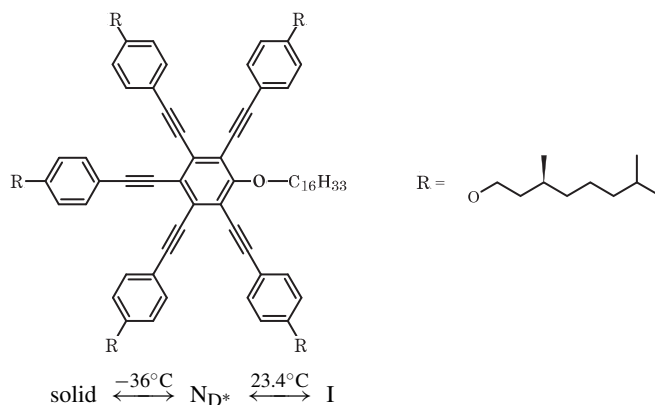


Figure 1.43 The molecular structure and transitions of a chiral discotic nematic mesogen [Langner et al., 1995].

is interesting to realize that the liquid crystal is formed by the combination of molecules not necessarily mesogenic by themselves.

Chiral discotic nematic, N_{D}^* , are also fairly rare. However, an example [Langner et al., 1995] is shown in Fig. 1.43.

1.10.1 Columnar LC Properties

Columnar liquid crystals are particularly promising as semiconductors for organic electronic applications [Sergeyev et al., 2007; Bisoyi and Kumar, 2010; Kaafarani, 2011]. Liquid crystals are typically insulators in the isotropic phase, with charge mobilities of the order of $10^{-5} \text{ cm}^2/(\text{V s})$ like the majority of organic compounds. However, as the molecular organization changes from isotropic to columnar by lowering the temperature, the charge mobility increases by more than two orders of magnitude, as we see in Fig. 1.44. Note from the figure that the mobility is even higher in the crystalline phase, but the values refer to a nearly ‘perfect crystal’, while in practice it is difficult to avoid structural defects that considerably lower the performance in the crystal phase. These defects, or *grain boundaries* where different orientations of the crystal domain clash, can instead be avoided by the fluidity and self-healing capabilities typical of the liquid crystals, even in the rather stiff

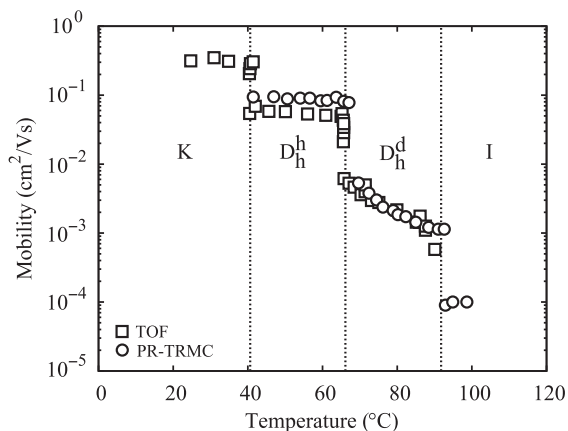


Figure 1.44 Charge mobility data of positive carriers in HHTT measured by time of flight (TOF) and pulse-radiolysis time-resolved microwave conductivity (PR-TRMC) [Warman and Van de Craats, 2003]. The dotted lines represent phase transitions.

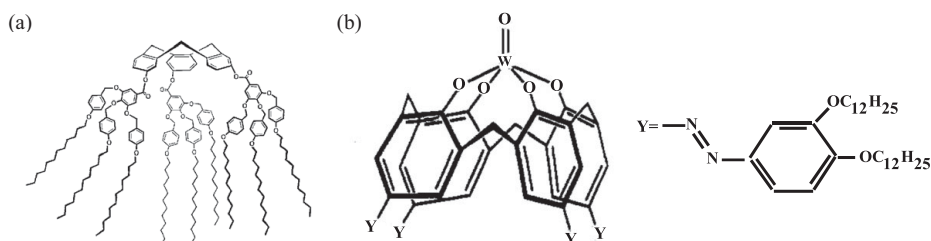


Figure 1.45 Two pyramidal molecules: (a) a fully organic one [Malthête et al., 1989] and (b) an organometallic one [Xu and Swager, 1993].

columnar phase. Another interesting feature is that the conductivity is strongly anisotropic, mainly directed along the columns, where the distance between the electron rich cores is of around 3.5–3.8 Å, the typical ‘thickness’ of a π -electron system, while the separation between the columns is, for HHTT, of around 20 Å. Even if this intercolumnar distance depends of course on the lengths of the chains and on the bulkiness of the substituents, it is so large anyway to reduce intercolumnar charge hopping, leading to strong conductivity anisotropy.

Other potential applications of columnar liquid crystals can be found in organic light-emitting diodes (OLED) [Benning et al., 2000] or in organic solar cells [Idé et al., 2014].

1.10.2 Bowlic Liquid Crystals

An interesting family of liquid crystals has been realized from bowlic or pyramidal shaped molecules, as, for example that in Fig. 1.45a, which is formed by a cone-shaped tribenzocyclonene (TBCN) core with three flat triangular substituents 3,4,5-tris-(*p*-*n*-dodecyloxy

benzyloxy) benzoyloxyl (DOBOB) groups [Malthête et al., 1989]. This particular compound forms a single hexagonal columnar phase stable up to 145–150°C. Organometallic type molecules of this category have also been synthesized using a metal like tungsten or vanadium in a suitable hybridization state to orient its ligands in some appropriate directions [Xu and Swager, 1993; Atwood et al., 2001], like in Fig. 1.45b. Other bowlic mesogens have been put forward, e.g. based on tribenzocyclononenes [Zimmermann et al., 1985], cyclovtryveratrilene [Cometti et al., 1992], calix[4]arenes [Demus, 1989; Swager and Xu, 1994], and C₆₀ fullerene molecules [Sawamura et al., 2002]. In the latter case, the C₆₀ apex of each of these molecules fits perfectly into the cavity of a neighbouring one. These molecules can pile up in columns, similar to what discotics do, but with the important difference that the constituent particles are intrinsically asymmetric and that the stacking might preserve and enhance this asymmetry, yielding an overall polarity of the column. For a molecule with an axial dipole, like that of the mesogen in Fig. 1.45b, this offers in principle the possibility of creating simple ferroelectric fluid systems. Indeed, it can be shown, if the columns are arranged in a hexagonal structure [Guillon, 2000], that the dipole of overall polar individual columns cannot be balanced, for symmetry reasons, by that of an equal number of antiparallel columns with the result of obtaining a much sought-after ferroelectric columnar phase. Unfortunately, this objective, although not forbidden by some fundamental law, has not been realized, at least as yet.

1.11 Lyotropics

1.11.1 Micelles

We consider now phases, generically called *lyotropics*, formed by amphiphilic molecules A-B consisting of two parts A and B with different affinity to a certain host solvent C (see Fig. 1.46). A classic example is that of elongated molecules formed by lyophilic and lipophilic parts dissolved in a polar solvent (typically water) [Linden and Fox, 1975; Wennerström and Lindman, 1979; Tiddy, 1980; Charvolin and Hendriks, 1985; Seddon, 1990; Figuereido Neto and Salinas, 2005; Fong et al., 2012]. When the solvent C is water, common amphiphilic molecules (also called *surfactants*) can be classified as:

- *Anionic* – with a negatively charged hydrophilic group carboxyl (RCOO⁻ M⁺), sulphonate (RSO₃⁻ M⁺), or sulphate (RSO₄⁻ M⁺).
- *Cationic* – with the hydrophile bearing a positive charge, as for example, the quaternary ammonium halides (R₄N⁺ X⁻).
- *Non-ionic* – where the hydrophilic moiety has no charge but derives its water solubility from highly polar groups such as polyoxyethylene (POE) (–OCH₂CH₂O–), sugars or similar groups.
- *Amphoteric* (and *zwitterionic*) – in which the molecule is neutral overall, but has both a positive and a negative charge on its structure as, for instance, for the principal chain of the sulphobetaines (Fig. 1.46f), instead of needing a separate counterion.

A simple example of a system of the first or second kind is a soap-water mixture. The amphiphilic molecules tend to organize themselves so as to segregate the hydrophobic

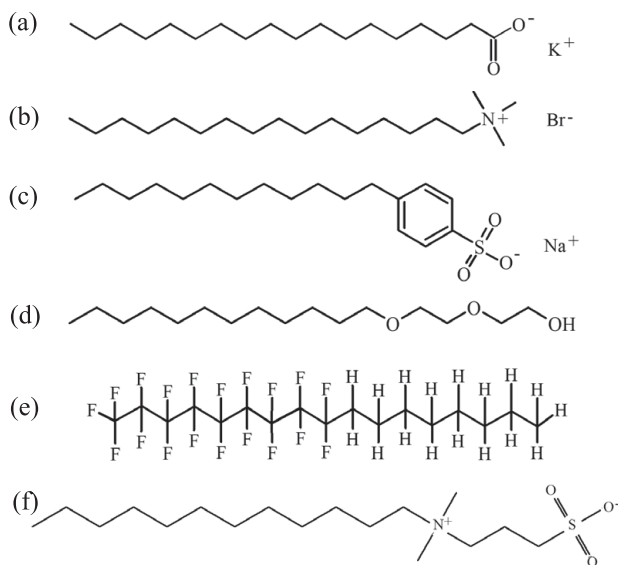


Figure 1.46 Some common water-soluble amphiphilic molecules: (a) potassium stearate (aliphatic, anionic); (b) cetyltrimethylammonium bromide (CTAB) (aliphatic, cationic); (c) sodium *p*-dodecyl benzene sulphonate (partly aromatic, anionic); (d) di (ethylene glycol) dodecyl ether (non-ionic); (e) a fluorinated-protonated amphiphile; (f) a zwitterionic molecule: lauryl sulphobetaine.

chains from the water. Different molecular arrangements occur, depending on the chemical structure of the amphiphile and on its concentration, as we see in Fig. 2.28 for potassium stearate, a typical example of these soaps [Luzzati et al., 1957].

When a certain critical micellar concentration (*CMC*) is reached, globular aggregates exposing the hydrophilic part of the molecule to the solvent, while having chains with a favourable reciprocal interaction on the inside (*micelles*), can be formed. The *CMC* of amphiphilic molecules with a net charge is normally very low (e.g. around 8 mM for SDS, sodium dodecyl sulphate [Wennerström and Lindman, 1979]), but strongly influenced by the ionic strength of the medium that acts, through a charge screening, towards dampening of the electrostatic repulsion between the ions. For instance, the *CMC* of the detergent sodium dodecyl sulphate is reduced tenfold when the NaCl concentration is raised from 0 M to 0.5 M. The shape of the micelles themselves can vary, as we sketch in Fig. 1.47, in order to optimize the local curvature, e.g. when we have a mixture of different amphiphiles where the size of the polar heads and of the chain lengths change [Israelachvili, 1992].

Spherical micelles. The simplest system is that of a suspension of isolated spherical micelles (Q phase). The polar heads are outside if the solvent is a polar one. The chains are directed toward the centre, although an arrangement that avoids excessive steric hindrance has to be found showing that the model in Fig. 1.47 can be too simple. Increasing the concentration of amphiphilic molecules in water means micelles come in contact and various structures can be formed. The diameter of these micelles is close to two molecular

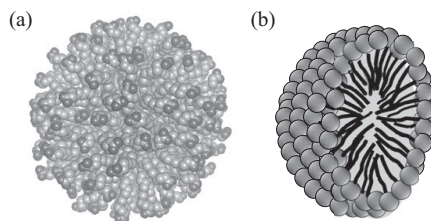


Figure 1.47 An atomistic representation of (a) a spherical micelle and (b) an idealized cartoon rendering of its section.

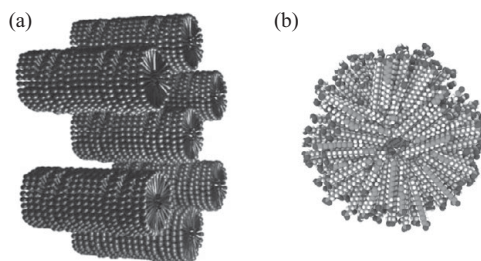


Figure 1.48 (a) Sketch of the hexagonal phase of cylindrical micelles and (b) of a section orthogonal to the micelle axis.

lengths (thus a few nanometres) and the connected high surface curvature is favoured by a cone-like molecular geometry typical of a polar head larger than the chain cross section.

Elongated micelles. Elongated micelles, e.g. cylindrical ones, can organize themselves so as to form, in turn, ordered structures. In Fig. 1.48 we see a sketch of the hexagonal, H, (also called *middle*) phase. All the phases we have seen have polar heads in contact with the solvent and inside chains, even though *reverse micelles* with chains pointing outside towards the solvent could be formed by suitably changing from water to a hydrophobic solvent [Tiddy, 1980]. More complex molecular architectures can be obtained increasing the concentration of amphiphiles so that micelles come into contact with each other [Luzzati et al., 1968].

Micellar architectures. Cubic arrays of spherical micelles can be obtained, e.g. with palmitoyl lysophosphatidyl choline (PLPC) [Landau et al., 1997]. In Fig. 1.49, we see instead an example of a so-called I (intermediate) or *cubic phase*, where the target of separating the immiscible water and lipid regions is met with a *fusion* process of the individual aggregates forming regular arrays of bilayer micellar units with a rather fascinating bicontinuous organization with water outside. In these systems a lipophilic solute molecule, e.g. a dye, should be able to migrate through all the sample without ‘getting wet’, so to speak. Phases of this type, e.g. 1-mono palmitoleoyl-*rac*-glycerol (MOG) have proved to be particularly useful in assisting the crystallization of proteins [Landau and Rosenbusch, 1996; Landau et al., 1997]. Note that, although the local surrounding of one of the mesogenic molecules is anisotropic, the overall macroscopic cubic symmetry gives optical isotropy to these phases

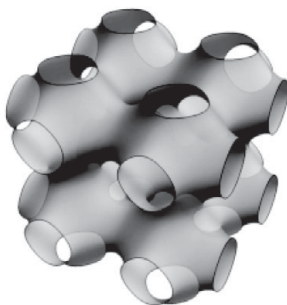


Figure 1.49 A bicontinuous cubic lyotropic phase of type I obtained by replicating the double layer micellar unit with water outside the structure as well as in the network channel inside.

that have the physical aspect of highly viscous, transparent materials. Other types of cubic phases, typically obtained from lipid bilayers, are based on a tetrahedral repeating unit and are denoted G (the *gyroid* type) and D (the diamond type) [Kulkarni, 2012].

Templating. In terms of applications, the ordered micellar arrangements are particularly important as templates in sol-gel synthesis of materials with a well-ordered and regular nanoporous structure [Raimondi and Seddon, 1999; Soler-Illia et al., 2002]. In practice, an organosilicate like tetraethyl orthosilicate (TEOS) that can hydrolyze and yield silica in the presence of water is added to the lyotropic system with the result of embedding the micelles in a silica matrix. A calcination is then performed, burning out the amphiphile forming the micelles, thus leaving empty nanopores. The extraordinary thing is that when performed with due care this rather invasive sequence of processes preserves the former micellar structure, leaving a solid nanoporous material with the original architecture [Attard et al., 1995]. Note also that the diameter of the spherical or cylindrical nanopores can be varied changing the chain length of the starting amphiphiles, providing a way of tuning the size of the cavities of these artificial zeolites and their effect on the molecules trapped inside, like significantly altering the melting point of water confined inside (see, e.g., [Findenegg et al., 2008]). The soft-templating methodology has been much extended and mesoporous (2–50 nm pore size) materials of many compositions beyond silicates, e.g. polymers, carbons, metals, metal oxides and of different dimensionality, have been prepared [Zhao et al., 2019]. Templating and fabrication applications are not the only available for lyotropics LCs and many others are used in drug delivery, as discussed, for example, by Chen et al. [2014].

1.11.2 Lamellar Phases, Bilayers and Membranes

Bilayer structures, like those shown in Fig. 1.50, with the chains separated from the water by the polar heads often form at higher amphiphile concentrations. *Lamellar phases* are similar to smectics, in having a one-dimensional periodic structure, but numerous organizations exist, corresponding to different arrangements of the chains. This variety has even caused some confusion in their nomenclature. Here we shall try to base our notation on the system

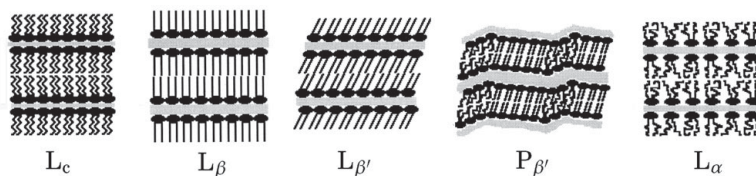


Figure 1.50 Cross-sectional sketch of some of the main bilayer phases. From the left: subgel (L_c), gel with untilted chains (L_β), gel with tilted chains ($L_{\beta'}$), rippled gel ($P_{\beta'}$) and liquid-crystalline fluid (L_α) [Koynova and Caffrey, 1998].

initially proposed by Luzzati [Tiddy, 1980] where a code name is built using a capital letter for the phase type: L for (planar) lamellar, H for hexagonal and Q for spherical micelles, then roman numerals I, II to denote normal and reverse structures, if this needs to be specified [Seddon and Templer, 1993]. A subscript α is used to indicate, where appropriate, a fluid, liquid-like, while β is for a gel, solid-like, state of the molecular chains in the layers, and c for a solid-crystalline chain organization. In addition, the label γ indicates a phase with a sequence of α and β layers.

The tilt of the chains is indicated by adding a prime to the α , β or γ subscripts. For instance, the lamellar, hexagonal and reversed hexagonal illustrated earlier on could be called L_α , H_I and H_{II} . The L_α phase, also called liquid crystal, or *neat phase* in soap-water systems, has a fluid like organization of the chains above a certain temperature (*Kraft point*) but below it forms gels with networks of lamellar domain. *Coagels*, consisting of hydrated crystalline phases [Lo Nostro et al., 2003], also form. When the lamellar phase is rippled rather than just flat it is called P instead of L. Lamellar phases have a flat interface with water having a negligible curvature and they are more easily obtained from amphiphiles with nearly cylindrical overall shape. This is typically obtained with amphiphilic molecules with two chains attached to the polar head, like in the phospholipids that are the main constituents of biological membranes. By contrast, we may remark that the various spherical or cylindrical micelles that we have discussed until now are, typically, formed by a relatively large polar head and a single chain, that confer an overall cone-like, rather than cylinder-like shape to the amphiphiles [Israelachvili, 2011]. Upon shaking up a lamellar water suspension, the bilayers, particularly the phospholipid made ones, tend to close up upon themselves forming spherical vesicles like those shown in Fig. 1.51. These can be *monolamellar*, as in Fig. 1.51a, with diameter of 25–30 nm if the suspension is shaken at length with ultrasound (sonicated). Otherwise *multilamellar smectic* structures, with various bilayer shells, disposed onion-skin-like called *liposomes* [Deamer, 2010], are obtained. It is worth stressing that although liposomes can appear similar, at first sight, to spherical micelles, they are very different, as they have a water pool inside and their size is more than two orders of magnitude larger. Multilamellar liposomes typically range in diameter from 0.1 to 5 μm [Mabrey-Gaud, 1981] and are characterized by temperature dependent reversible order-disorder transitions occurring in a narrow temperature range. Multilamellar vesicles represent a more stable state with respect to the single layer ones and freshly prepared unilamellar vesicles tend

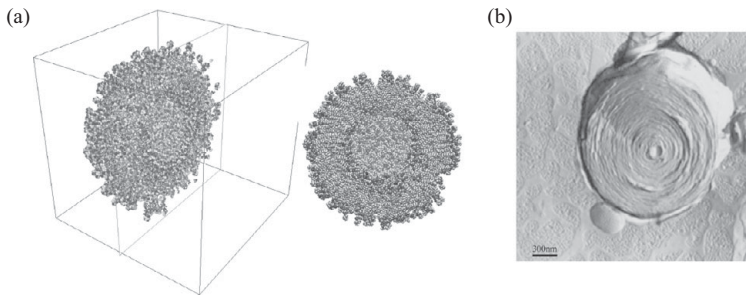


Figure 1.51 (a) Perspective and front view of an atomistic sketch of monolamellar vesicle (section). (b) A freeze fracture electron microscopy of 1,2-dioleoyl-sn-glycero-3-phosphocholine (DOPC) multilamellar liposomes [Francescangeli et al., 2003].

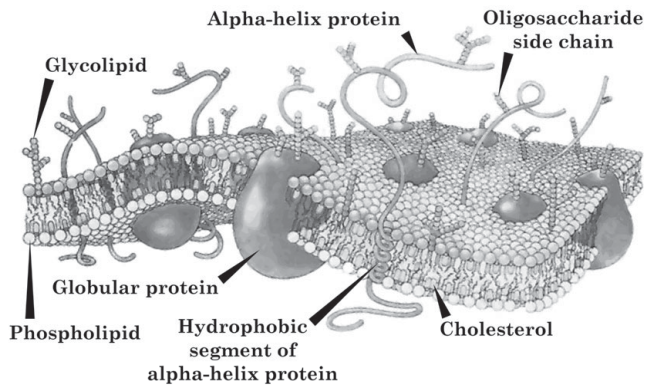


Figure 1.52 The fluid mosaic model of a cell membrane showing the liquid-crystalline organization of the lipids and the transmembrane proteins. The bush-like structures shown on the top are glyco-proteins [NIST Center for Neutron Research, 2016].

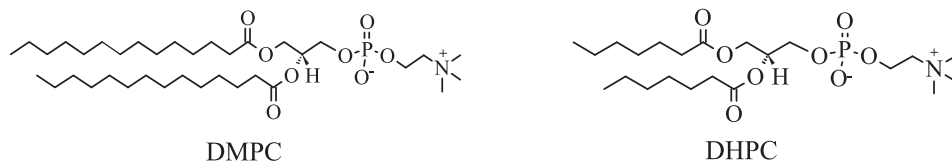
to fuse and give rise to multilamellar liposomes [Suurkuusk et al., 1976]. We also note that, although liposomes are macroscopically isotropic, they have local orientational order. Thus, they can show the same properties in every direction when a methodology probing at a macroscopic level, e.g. a rheological method to determine viscosity, is used and can appear ordered when a spectroscopic technique probing the structure at a local, molecular level is employed instead [Zannoni, 1981]. The bilayer structure common in phospholipid systems [Mabrey-Gaud, 1981] is particularly important because it models the organization found in the real membrane surrounding a cell. It is indeed similar to the ‘enclosing envelope’ of a eukaryote animal cell (see Fig. 1.52), i.e. a cell of an organism where a membrane encloses nucleus, mitochondria and other membrane bound organelles [Brown and Wolken, 1979; Lehninger et al., 2005]. The lipid cell membrane, called the *plasma membrane*, is of great biomedical importance because it is necessarily involved in the transport of chemicals and ions to and from the cell. The current, textbook, model for these lipid biomembranes is the

fluid mosaic model [Singer and Nicolson, 1972] sketched in Fig. 1.52. In essence, it is based on a lipid double layer, with globular proteins embedded inside or going across the bilayer itself.

The amount of proteins, lipids and other components varies from system to system. In red blood cells membrane proteins constitute 60%–70% of the total dry weight, with lipids making up 20%–40%. Note that the microscopic organization of the membrane bilayer is essentially that of a liquid crystal. The influence of the state, e.g. the order and fluidity of the lipids on the properties of the membrane is a topic of great current interest. To complicate the picture, in a real membrane the lipids themselves are mixtures of many different kinds, so that we can have other phenomena like separation (segregation) of the various components in certain thermodynamic conditions. As already mentioned, phospholipids are typical components of the bilayer and artificial membranes can be prepared from them. In particular, model systems like dimyristoyl-phosphatidyl choline (DMPC) and dipalmitoyl-phosphatidyl choline (DPPC) have been very well studied experimentally (see Section 2.14) and with computer simulations (Section 12.7.2).

1.11.3 Discoidal Micelles and Bicelles

Nematic lyotropics can be formed by discoidal micellar units. A nematic lyotropic system of this type, with a structure similar to that shown in Fig. 1.39a can be obtained, for example, with 30.35% potassium laurate (KL), 7.04% decanol and 62.61% water at a temperature of 17°C [Charvolin and Hendriks, 1985]. Discotic bilayer micelles, sometimes called *bicelles*, [Sanders and Landis, 1995] can be prepared from suitable mixtures of phospholipids of different length. For instance, a mixture of dihexanol phosphatidylcholine (DHPC) and dimyristoyl phosphatidylcholine (DMPC) in aqueous solution at room temperature or just above goes from gel to a liquid crystal formed of bicelles of thickness ≈ 4 nm [Sanders and Schwonek, 1992] that has proved to be particularly useful as a solvent of weak and tunable anisotropy for Nuclear Magnetic resonance (NMR) studies of biomolecules, where they provide an environment similar to that of real biomembranes [Tjandra and Bax, 1997].



It seems that in these systems a disc-like phospholipid bilayer formed by the longer chains (DMPC) is surrounded by a rim of the short chain lipids (DHPC). In a magnetic field these bicelles align with the disc axis, i.e. the bilayer normal, perpendicular to the field, although the addition of small amounts of lanthanides ions (e.g. Eu^{3+}) changes the alignment of the axis to being parallel to the field [Vold and Prosser, 1996]. The radius of the bicelles increases from roughly 1 nm to 100 nm as the ratio of DMPC to DHPC increases from 0.01 to 100.

While we have discussed up to now thermotropic systems that change molecular organization by varying temperature and lyotropics, where transformations are driven by modifications in composition of a solution, a number of systems, particularly natural ones, are amphitropic, in the sense that they show both types of behaviour. Phospholipids are an example [Chapman, 1975], phthalocyanines [Eichhorn et al., 1998] and many sugars are others [Blunk et al., 2009; Hashim et al., 2012].

1.12 Chromonics

Chromonics [Lydon, 1998, 2004] are a kind of lyotropic system but, differently from those seen until now, they are formed dissolving in water amphiphilic mesogens (ionic or non-ionic) that typically have an aromatic structure, with a fairly rigid and planar disc-like or plank-like core (Fig. 1.53), instead of the aliphatic, flexible, and elongated shape of common lyotropics. These mesogens have their polar, hydrophilic groups disposed around the periphery of the molecules rather than at one end. The molecules form one-dimensional stacks of various length in solution, without a critical concentration, rather than zero-dimensional (closed on themselves) micelles. The face-to-face aggregates can form a disordered nematic phase (Fig. 1.54a), but also more ordered arrays of columns, in particular, various hexagonal (H) phases (see, e.g., Fig. 1.54b). In the hexagonal phases the columns lie in a somewhat hexagonal array, differently from the more dilute nematic N phase where the columns are separated by a larger water amount. Some of these materials are in use as food dyes, and their suggestive common names (Fig. 1.53, caption) are inherited from that area. Chromonics are also used for optical devices, where a common orientation of the liquid-crystalline columns

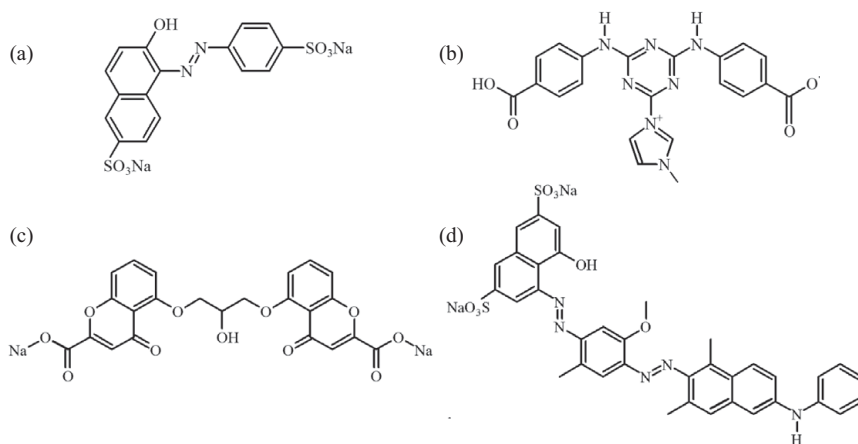


Figure 1.53 Some common chromonic mesogens: (a) 6-hydroxy-5-[(4-sulphophenyl) azo]-2-naphthalenesulphonic acid, also called Sunset Yellow (SSY) or Edicol [Edwards et al., 2008]; (b) 3-[6-(3-carboxyanilino)-4-(3-methyl-1H-imidazol-s-ium-1-yl)-1,3,5-triazin-1-ium-2-yl] aminobenzoate or just *n*-methyl imidazol (NMI) [Mohanty et al., 2006]; (c) disodium cromoglycate (DSCG), also called Cromolyn or Intal and (d) Direct Blue.

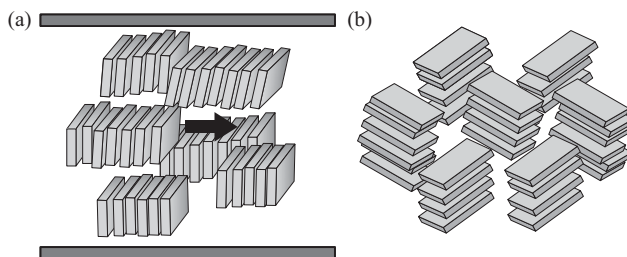


Figure 1.54 A sketch of a chromonic nematic (N) with (a) its columnar stacks aligned by flow in the direction of the arrow and (b) of a hexagonal (H) chromonic phase.

is achieved by a mechanical shearing force. Successive evaporation of the solvent can result in anisotropic solid films that can, e.g. linearly polarize incident light over a rather wide interval of wavelengths. If the columns are aligned parallel to the shearing direction (see Fig. 1.54a), the direction of the absorption transition moment (see Section 3.4.2 for the aromatic cores would typically be in the plane of the molecule, so that the component of an unpolarized light incident on the film with polarization along the stacks will be transmitted and the component with polarization perpendicular to it will be well absorbed.

It is interesting that the elastic constants of chromonics are rather different in relative magnitude from those of nematics. While in simple nematics K_{11} , K_{22} and K_{33} have values comparable to each other (see Table 1.3 and Fig. 1.26), in chromonics the twist constant K_{22} is nearly an order of magnitude smaller than the other two. For instance, for Sunset Yellow at a concentration of 29%, Zhou et al. [2012] found $K_{11} = 4.3 \pm 0.4$ pN, $K_{22} = 0.70 \pm 0.07$ pN and $K_{33} = 6.10 \pm 0.06$ pN.

1.13 Ionic Liquid Crystals

Thermotropic ionic liquid crystals [discussed in detail in Binnemans, 2005; Axenov and Laschat, 2011; Salikolimi et al., 2020] are a class of liquid-crystalline compounds typically obtained from anisotropic organic salts. Their defining property stems from being constituted of anions and cations, making them quite different from ordinary thermotropics, and it is not surprising that various of their properties, particularly their ion conductivity, differ significantly from those of conventional liquid crystals. Like ordinary, isotropic, ionic liquids, these compounds have a very low vapor pressure and thus low volatility. The ionic interactions tend to stabilize smectic-like lamellar mesophases. Most of the systems studied so far are imidazolium-derived ionic liquid crystals [Axenov and Laschat, 2011], as we see in Fig. 1.55. In the first type (Fig. 1.55a), the imidazolium group acts as a mesogenic core, which is substituted by one or multiple long aliphatic tails. In most of such cases, alkyl substituted imidazolium salts do not form nematics, but only smectic mesophases where the molecules are arranged in layers. This is due to the electrostatic interactions in the head group region and to the weaker van der Waals forces in the hydrophobic tails (see Chapter 5). The imidazolium group could also be connected via a flexible spacer to a conventional liquid

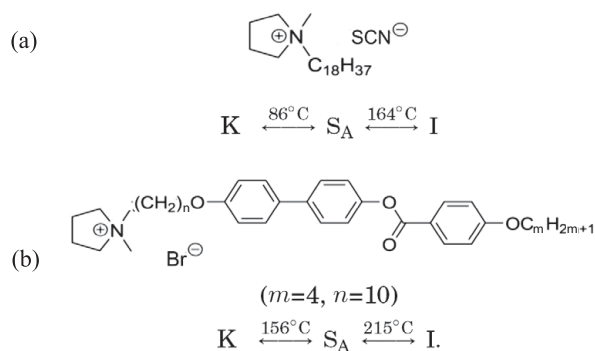


Figure 1.55 Some imidazolium-based ionic liquid crystal [Axenov and Laschat, 2011].

crystal mesogen on the tail ends (Fig. 1.55b). In these types of imidazolium-based materials, the liquid-crystalline properties originate from their strong amphiphilic character. The ionic interactions of the imidazolium groups stabilize both S_A and S_E phases. However, some imidazolium units with two pendant cyano-biphenyl groups show a monotropic nematic [Goossens et al., 2008]. Stable columnar phases have been obtained for the compounds, where imidazolium groups have been attached on the tail ends of discotic molecules.

A series of salts with two mesogenic cyano-biphenyl groups attached to a central pyridinium cationic unit via a flexible alkyl spacer was instead shown to exhibit only a nematic phase with a thermal range influenced by the various counterions employed and spacer length [Pana et al., 2016].

1.14 Colloidal Suspensions

An interesting and increasingly important [Mitov, 2012; Mušević, 2017] set of liquid crystals is obtained from suspensions of anisometric colloidal particles, where one or more of their dimensions is nanometric to micrometric in size. For particles up to this range of sizes the effects of gravity can, to a good approximation, be neglected and various isotropic and anisotropic phases [Manoharan, 2015] can be observed as a result of the balance between attractive forces leading to some sort of aggregation and repulsive forces tending to stabilize the suspension. These forces will be examined in Chapter 5, while for now we just wish to mention that the particles in liquid-crystalline suspensions can be of inorganic, mineral, polymeric or even biological origin. Amphiphilic particles (anisotropic Janus particles) can also be studied [Conradi et al., 2009]. For all these suspensions a very direct evidence of the formation of a liquid crystal is the observation of light transmission through crossed polarizers, due to the onset of anisotropy (see Fig. 1.56). Let us briefly examine the main types.

Mineral colloids. Classic examples are suspensions of particles of mineral origin [Davidson and Gabriel, 2005; Lekkerkerker and Vroege, 2013], e.g. rod-like bohemite (AlOOH) [Buining et al., 1994] or platelets of gibbsite ($\gamma\text{-Al}(\text{OH})_3$) in toluene [van der Kooij et al., 2000].

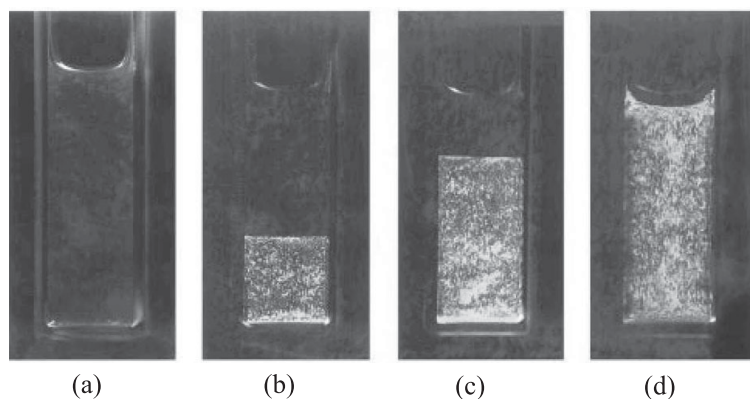


Figure 1.56 The formation of an anisotropic nematic in a suspension of platelets as their volume fraction increases from (a) to (d) monitored by the transmission through crossed polarizers due to the onset of birefringence [van der Kooij and Lekkerkerker, 1998].

In Fig. 1.56 we see such an example for a suspension of platelet shaped particles. Note that such a discotic nematic phase is obtained easily in colloidal suspensions, while it is extremely difficult to find it in thermotropic materials, where normally the transition is from isotropic to columnar upon cooling. It is also interesting that some of these suspensions convincingly appear to be biaxial nematics [Vroege, 2013], once again a phase very difficult to find, if at all, in thermotropic materials [Luckhurst and Sluckin, 2015].

Inorganic nanorods. Other liquid crystal assemblies (nematics and smectics) can be formed from suspensions of inorganic nanocrystals. In Fig. 1.57 we see an example of cadmium selenide nanorods from Alivisatos group [Li et al., 2002]. This is particularly interesting for semiconductor nanocrystals or *quantum dots* (QDs) in view of their optical absorption and fluorescence properties [Reed, 1993]. Indeed, when at least one of their sizes is in the range of a few nanometres, the quantum confinement is at the origin of fluorescence light emission at well-defined wavelengths depending on the particle size. Thus, a spherical or a rod-like QD can generate, in particular, a narrow red, green or blue emission band when illuminated with suitably UV light just choosing their diameter (for a sphere) or cross section (for a rod) to be of the appropriate size.

Note that the suspending host fluid does not have to be isotropic, but could be a liquid crystal. Indeed, novel hybrid systems have been obtained by Munder et al. [2018] using micron long, charged, inorganic colloidal nanorods of bare $\text{NaYF}_4:\text{Yb/Er}$, with length-to-diameter ratios of 40–110. These nanorods tend to align perpendicularly to the 5CB director and form uniaxial and biaxial nematic phases of the composite mixture. They present very interesting optical properties due to the upconverting properties of the lanthanide-doped nanorods that can absorb multiple photons in the infrared and emit in the visible [Wang and Li, 2007].

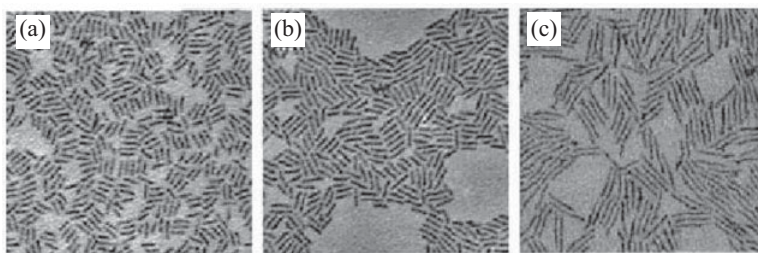


Figure 1.57 A liquid crystal suspension formed by CdSe nanorods of length (a) 11, (b) 20 and (c) 40 nm and width of ≈ 3.2 nm, respectively [Li et al., 2002].

Carbon nanotubes. Nematics can be formed by multiwall carbon nanotubes (CNT) in aqueous suspensions, e.g. CNT with average length ≈ 675 nm, average width ≈ 25 nm and concentration ≈ 4.8 vol% [Song et al., 2003a]. Single-wall nanotubes in strong acid suspensions [Rai et al., 2006] have also been studied.

Viruses. Viruses are of particular interest as model system of giant ‘molecules’ because, while being of colloidal size, each particle has the same length, diameter, mass and charge distribution, avoiding the polydispersity typical of other systems. This makes comparison with theory and computer simulations easier, eliminating the uncertainties and in general the effects due to an often unknown distribution of sizes and shapes. For instance, virus suspensions can form at a sufficiently high-volume fraction not only nematics, but also layered, smectic systems, that could be difficult to obtain from particles of different length. This was demonstrated in suspensions of tobacco mosaic virus (TMV) [Zasadzinski and Meyer, 1986; Dogic and Fraden, 2006] that, as shown in Fig. 1.58a and b, give nematic phases.

TMV is a plant virus, with rod-like shape [Caspar, 1964], 18 nm in diameter and 300 nm in length. TMV self-assembles from proteins and a single strand of RNA, ≈ 6000 nucleotides and ≈ 2130 copies of a single kind of polypeptide, the coat protein, each with 158 amino acids. The RNA forms a helical core, with a cylinder of protein subunits clustered around it. Another well-studied filamentous virus is *fd*. It has dimensions of about 880 nm in length and 6.6 nm in diameter. There are specialized proteins at the ends of the virus used for infection. The protein shell has a hollow core in the centre into which the DNA is contained and a helical coat, thus suspensions of *fd* virus are chiral nematics. Differently from TMV the virus is semiflexible, with a persistence length of 220–280 nm. *fd* as a virus is a bacteriophage that infects certain strains of *Escherichia coli* bacteria. Note that all the virus particles studied are strictly helical and thus chiral molecules. However, only some viruses form cholesterics (see Fig. 1.58c). Conventionally, when dealing with phases of nematic or smectic formed (as in Fig. 1.58d) the intrinsic chirality is neglected and they are considered effectively as achiral rods [Dogic and Fraden, 2006].

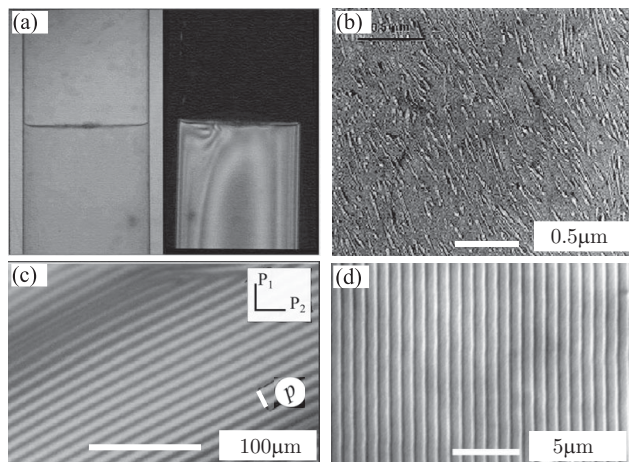


Figure 1.58 (a) Tobacco mosaic virus (TMV) water suspension, viewed between crossed polarizers, showing coexistence between the isotropic phase floating above the birefringent nematic one [Dogic and Fraden, 2006]. (b) Electron micrograph of a TMV nematic suspension [Gelbart and BenShaul, 1996]. (c) Image between crossed polarizers P_1 and P_2 of a *fd* virus cholesteric suspension phase. The pitch p corresponds to twice the repeat distance between the black stripes [Dogic and Fraden, 2000]. (d) Optical micrograph of a *fd* smectic. The *fd* particles lie in the plane of the photo with their long axis normal to the parallel lines (smectic layers). The layer spacing is $0.92 \mu\text{m}$. [Dogic and Fraden, 1997, 2006].

Large differences in elastic constants can be expected in liquid crystals originated from suspensions of long rod particles, e.g. virus like tobacco mosaic virus (TMV) [Hurd et al., 1985], nanotubes [Song et al., 2003a] or nanocrystal suspensions [Li et al., 2002].

1.15 Lyotropic Liquid Crystal Polymers

Polymer liquid crystals have become quite important for industrial applications since they can yield materials with extremely interesting mechanical properties. To quantify this, we recall that in a tensile stress-strain test an increasing force per unit area, the *tensile stress* Σ , is applied to a specimen and the resulting changes in length (*strain* λ) are measured. For a small applied force the behaviour of the material is elastic, with the sample recovering its original shape when the stress is released and $\Sigma = E_Y \lambda$, the classical Hooke's law of springs, holds. This initial slope E_Y is called *Young's modulus* or tensile modulus. Upon pulling the specimen, a maximum load is reached before the sample develops a 'neck' and *tensile strength* is defined as the maximum load over original cross-section area. Let us consider, as an example, one of the most commonly used liquid crystal polymers, Kevlar (du Pont[®]), a para-substituted aromatic polyamid (aramid), whose structure is

Table 1.8. Values of Young's modulus and tensile strength for some engineering materials [Anderson et al., 1990; Collyer, 1990]

Material	Young's modulus, E_Y (GPa)	Tensile strength (MPa)
Polyamide 66	3	80
Polyamide 66–30 vol.% glass fibre	8	160
Vectra (thermotropic LCP)	10–40	140–240
Aluminium	71	80
Ultradrawn polyethylene	117	3670
Kevlar (LCP fibre)	139	2700
Mild steel	210	460

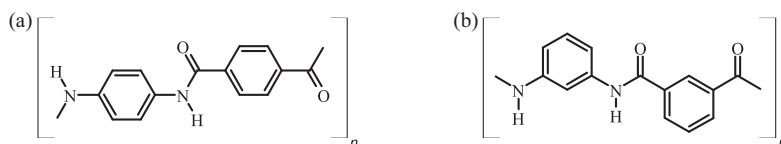


Figure 1.59 Chemical structure of two LCP. (a) Poly-para-phenylene terephthalamide or Kevlar (DuPont[®]). (b) Poly-meta-phenylene isophthalamide or Nomex (DuPont[®]).

shown in Fig. 1.59a, prepared polymerizing *p*-phenylene-diamine and terephthaloyl chloride. This main-chain polymer has high viscosity and is practically insoluble in organic solvents and only yields to very strong acids. The lyotropic liquid crystal obtained dissolving it in sulphuric acid can be spun to produce high-performance fibres. Chain alignment favours hydrogen-bonded sheet structures with the molecules forming stacks disposed radially with the chain backbone along the fibre axis. The Young's modulus of Kevlar, $E_Y = 139$ GPa and its tensile strength, 2.7 GPa, outperform those of aluminium [Anderson et al., 1990; Collyer, 1990] and compare favourably with other materials (see Table 1.8). Another similar LCP is Nomex (Fig. 1.59b).

1.16 Liquid Crystal Elastomers

An elastomer (rubber) is, in general, a molecular network formed by polymer chains with a certain, relatively low (e.g. 10%), percentage of cross links between the strands. Rubbers owe their characteristic elastic properties to this peculiar structure. In a liquid crystal elastomer (LCE), mesogenic units are embedded in the network [de Gennes, 1974; Anderson et al., 1990; Benning et al., 2000; Warner and Terentjev, 2003; de Jeu, 2012; Ohm et al., 2012] as shown in Fig. 1.60. As a result of this connected mesogenic structure a significant *thermal actuation* can arise, with changes in the form factor of an LCE sample that take place as the temperature crosses the isotropic-liquid crystal transition of the mesogenic

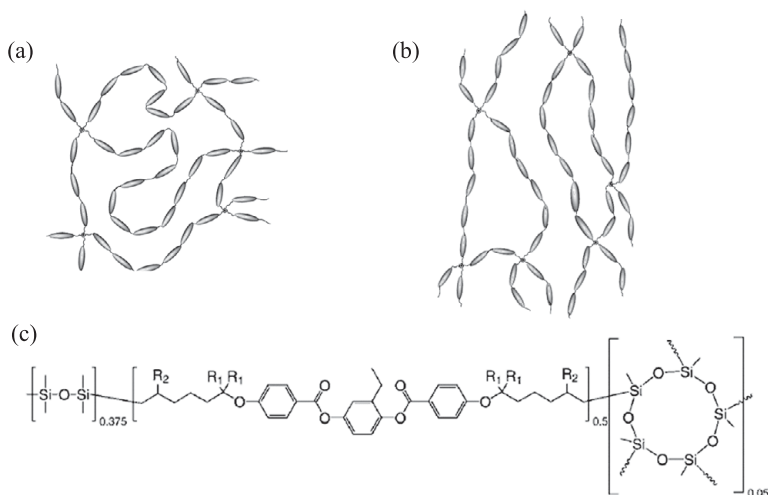


Figure 1.60 Sketch of a main-chain LCE in its (a) isotropic, disordered and (b) anisotropic, aligned nematic phase. (c) The chemical structure of a main-chain LCE [Brommel et al., 2011].

components. In Fig. 1.61a we report the actuation induced by temperature for four LCE materials from Finkelmann group and we see that elongation can change by as much as a huge 400%. Various ways have been proposed to achieve the temperature change in a localized region (a pixel) by dispersing graphite or carbon nanotubes in the LCE and illuminating the specific area [Torrás et al., 2013]. More generally, LCE unique mechanical properties are derived from the pronounced coupling between a macroscopic strain and the underlying mesogenic orientational order. As the latter can be controlled by a number of external stimuli [Ohm et al., 2012] beyond temperature, e.g. electric field, or ultraviolet light in the case of photo-responsive azobenzene-based elastomers, LCEs have great potential for application in various sensing devices, as well as for actuation. The potential applications of such actuators are fascinating, ranging from artificial muscles [de Gennes et al., 1997], heart valves, haptic displays [Torrás et al., 2013] and other biomedical applications, to micro- and nano-electromechanical devices like soft robots, as well as electro-optical systems like adaptive lenses, where their high deformability and low weight make them particularly promising. Among the possible actuation stimuli, the external electric field is particularly appealing, even if quite difficult to implement since a rather strong field is required to induce deformations. Side-chain [Finkelmann and Rehage, 1984] and main-chain [Ortiz et al., 1998; Donnio et al., 2000] LCEs have been prepared. Side-chain polymeric materials are somehow easier to prepare and treat, even if main-chain LCEs show the bigger actuation. Fig. 1.61b shows the unusual and very interesting stress-strain curve of a main-chain LCE at a few different temperatures. An initial stress gives a linear, Hookean behaviour, with a relative steep slope (stiff modulus) but then a flat plateau, corresponding to a large deformation obtained with nearly zero stress (supersoft elasticity), while a further increase in pulling

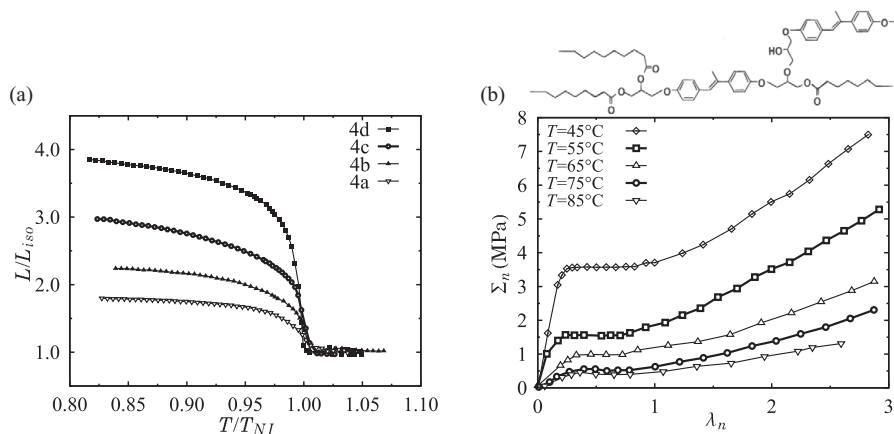


Figure 1.61 (a) The important elongation/contraction of monodomain LCE samples going through the NI transition, as shown by four different co-elastomer materials from Finkelmann group [Wermter and Finkelmann, 2001]. (b) The characteristic non-Hooke stress-strain trend, with a supersoft flat region of a main-chain LCE whose structure is shown above the stress-strain plot. Here Σ_n is the nominal or engineering stress (i.e. load divided by original cross-section area) and $\lambda_n = \Delta L/L$ is the applied nominal strain (i.e. deformation by unit length) [Ortiz et al., 1998].

gives again a normal Hooke behaviour. The phenomenon has been the object of intense theoretical study [Warner and Terentjev, 2003] and, recently, of computer simulations to be described later in Chapter 11 [Skačej and Zannoni, 2014].

1.17 Active Liquid Crystals

It is a common observation that many categories of living bodies show some sort of orientational if not positional order. On very different length scales, colonies of bacteria or fish shoals or flocks of birds or even herds of much larger animals are often spontaneously arranged in a manner far from disordered [Marchetti et al., 2013]. In particular, swarming and swimming represent instances of behaviour where motile bacteria migrate rapidly and collectively on surfaces. In many cases the constituent elements can be assimilated to rigid, self-propelled rods, but highly flexible, snake-like, active bodies, are also observed, like in the case of the strain of *Vibrio alginolyticus* shown in Fig. 1.62 [Böttcher et al., 2016].

It is worth noting that similar ordering effects take place not only in living systems endowed with some ‘intelligence’, but also in so-called active colloidal systems. A well-known case is that of Janus micron size colloidal particles [Ebbens et al., 2012; Jiang and Granick, 2012; Wang et al., 2015] with half body covered by a catalytic coating that reacts with the host solvent yielding a gas (in the classic example platinum coating and hydrogen peroxide solvent liberating oxygen).

Comparing all these, living or inanimate, systems with the anisotropic structures discussed until now for the various kinds of liquid crystals, it is apparent that some sort of LC

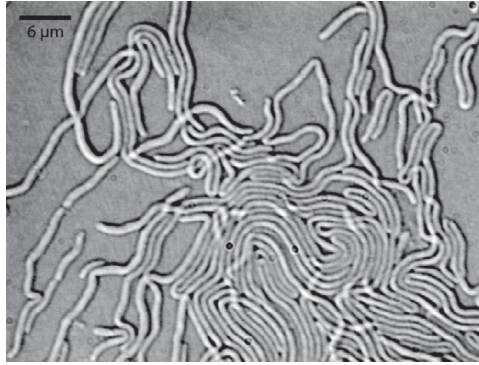


Figure 1.62 Swarming of a colony of snake-like *Vibrio alginolyticus* bacteria on a surface [Böttcher et al., 2016].

orientational order exists. There is, however, an important difference, since in all active systems the common characteristic is that the particles are propelled by some form of internal force and the resulting phases are thus not in equilibrium. The existence of an ordered state is dependent on the internal energy source (food, fuel or other) and can only persist until this is not exhausted. For reasons of space, we shall not treat in detail active systems in this book, even though the techniques discussed in this book will be of help in their microscopic description too.